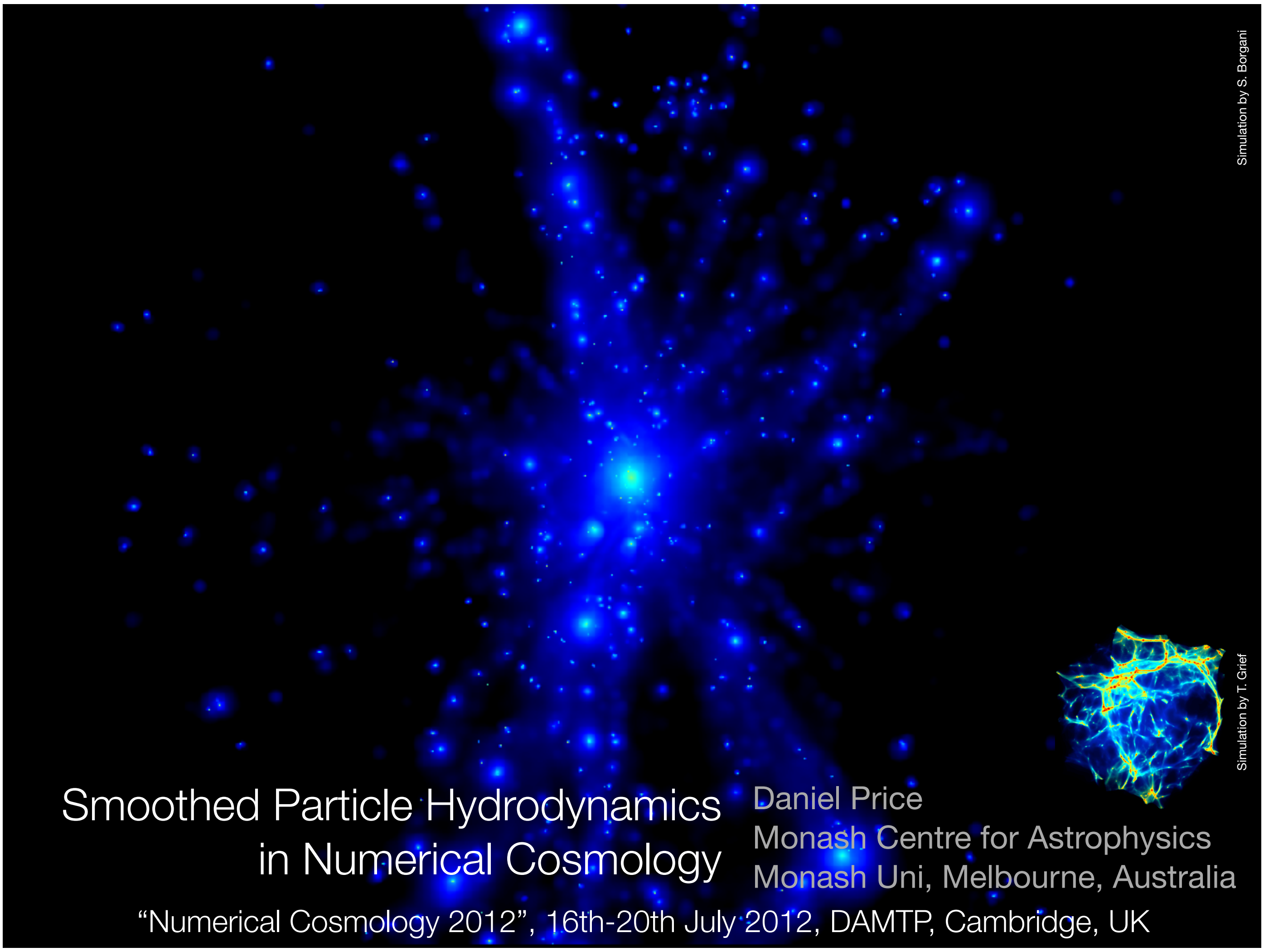

Smoothed Particle Hydrodynamics in Numerical Cosmology

Daniel Price
Monash Centre for Astrophysics
Monash Uni, Melbourne, Australia

“Numerical Cosmology 2012”, 16th-20th July 2012, DAMTP, Cambridge, UK

SPH starts here...

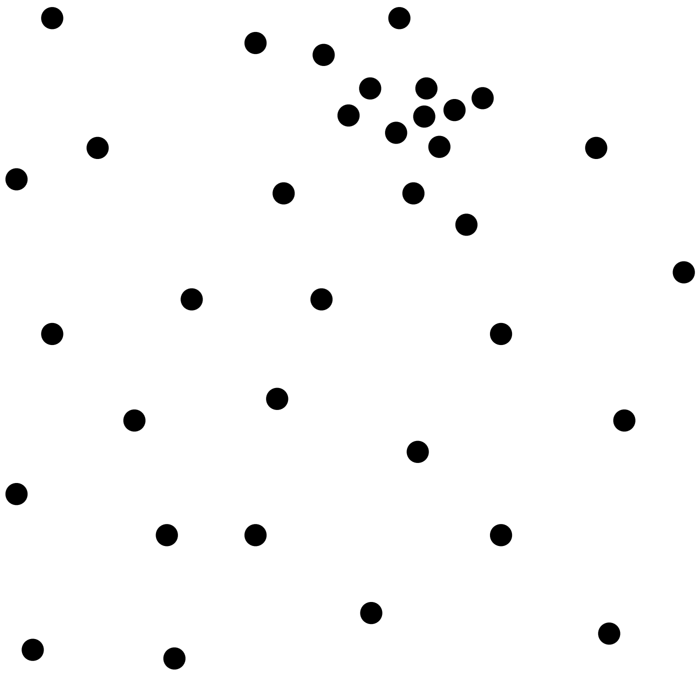

What is the density?

The SPH density estimate

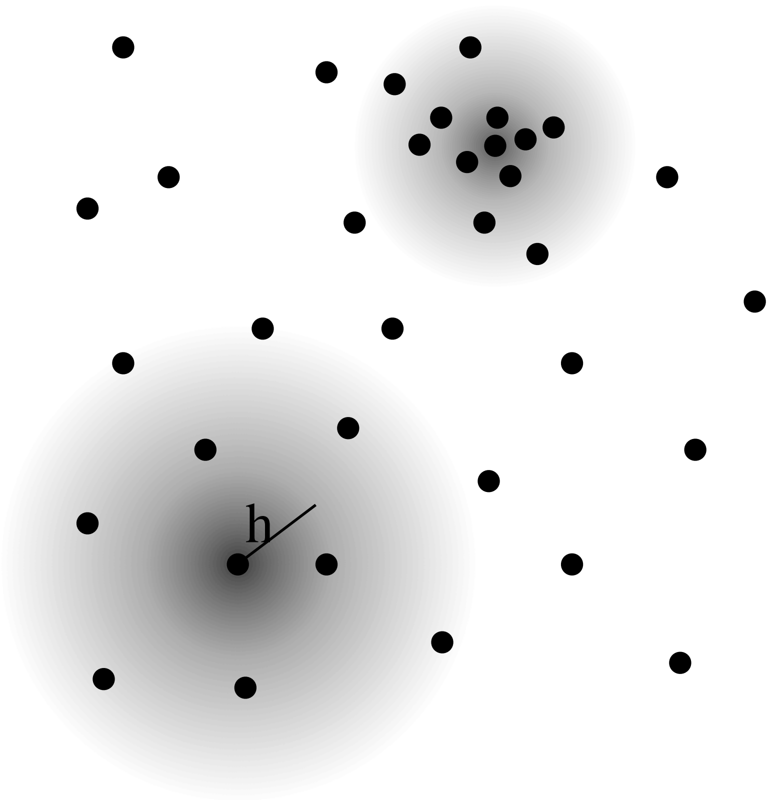

Kernel-weighted sum:

$$\rho(\mathbf{r}) = \sum_{j=1}^{N} m_j W(|\mathbf{r} - \mathbf{r}_j|, h)$$

e.g. $W = \frac{\sigma}{h^3} e^{-r^2/h^2}$

Resolution follows mass

Grid

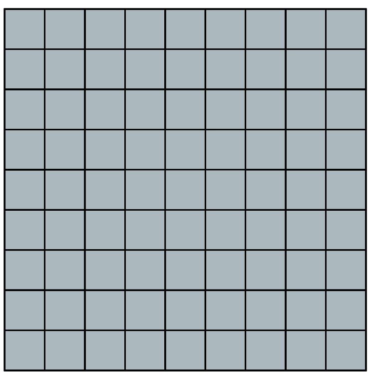

SPH

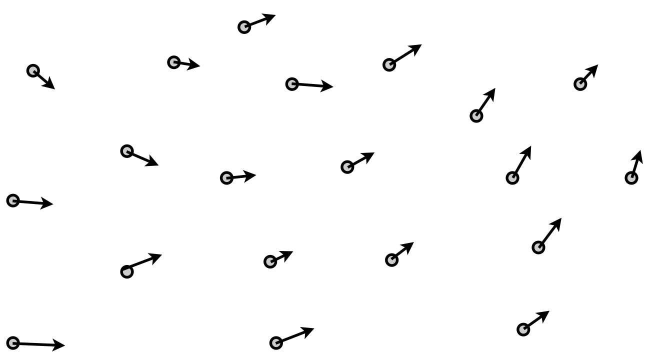

$$\frac{\mathrm{d}\mathbf{x}}{\mathrm{d}t} = \mathbf{v}$$

From density to hydrodynamics

$$L_{sph} = \sum_j m_j \left[\frac{1}{2}v_j^2 - u_j(\rho_j, s_j)\right]$$ ← Lagrangian

+

$$\mathrm{d}u = \frac{P}{\rho^2}\mathrm{d}\rho$$ ← 1st law of thermodynamics

+

$$\nabla\rho_i = \sum_j m_j \nabla W_{ij}(h)$$ ← density sum

+

$$\frac{\mathrm{d}}{\mathrm{d}t}\left(\frac{\partial L}{\partial \mathbf{v}}\right) - \frac{\partial L}{\partial \mathbf{r}} = 0$$ ← Euler-Lagrange equations

=

$$\frac{\mathrm{d}\mathbf{v}_i}{\mathrm{d}t} = -\sum_j m_j \left(\frac{P_i}{\rho_i^2} + \frac{P_j}{\rho_j^2}\right)\nabla_i W_{ij}(h)$$ ← equations of motion!

$$\left(\frac{\mathrm{d}\mathbf{v}}{\mathrm{d}t} = -\frac{\nabla P}{\rho}\right)$$

What this gives us: Advantages of SPH

- An exact solution to the continuity equation
- Resolution follows mass, natural compatibility with N-body codes
- ZERO dissipation
- Advection done perfectly
- EXACT conservation of mass, momentum, angular momentum, energy and entropy
- A guaranteed minimum energy state

Zero dissipation

Zero dissipation - Example I.

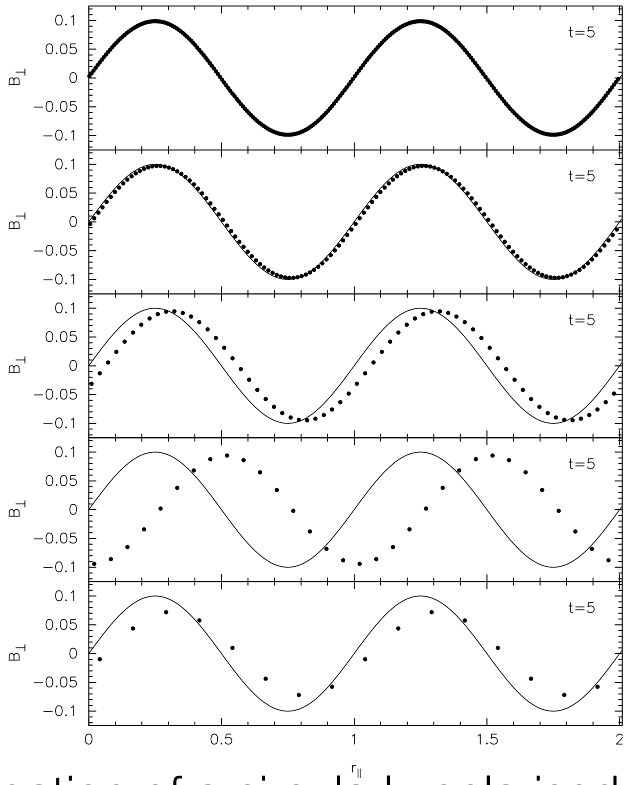

Propagation of a circularly polarised Alfven wave

Zero dissipation - II. Advection of a current loop

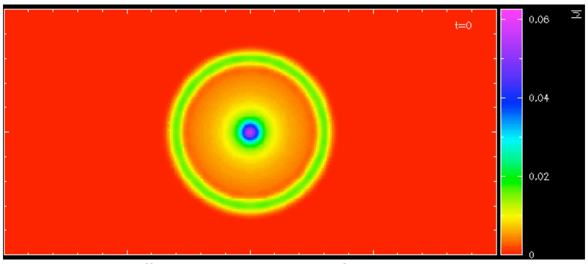

first 25 crossings

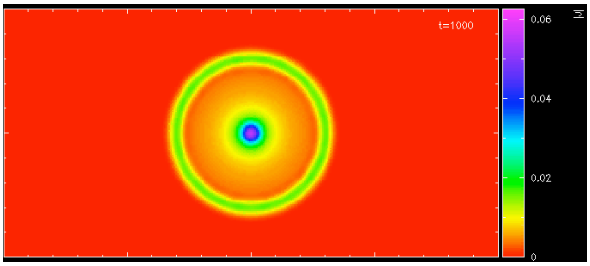

1000 crossings (Rosswog & Price 2007)

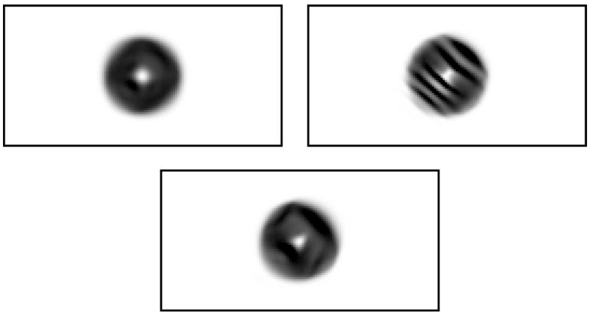

Fig. 3. Gray-scale images of the magnetic pressure $(B_x^2 + B_y^2)$ at $t = 2$ for an advected field loop $(v_0 = \sqrt{5})$ using the $\mathcal{E}_z^\alpha$ (top left), (top right) and $\mathcal{E}_z^c$ (bottom) CT algorithm.

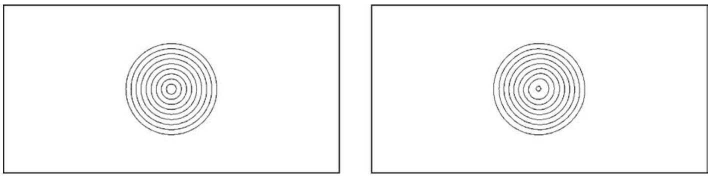

Fig. 8. Magnetic field lines at $t = 0$ (left) and $t = 2$ (right) using the CTU + CT integration algorithm.

2 crossings (Gardiner & Stone 2005)

SPH

grid

Zero dissipation...

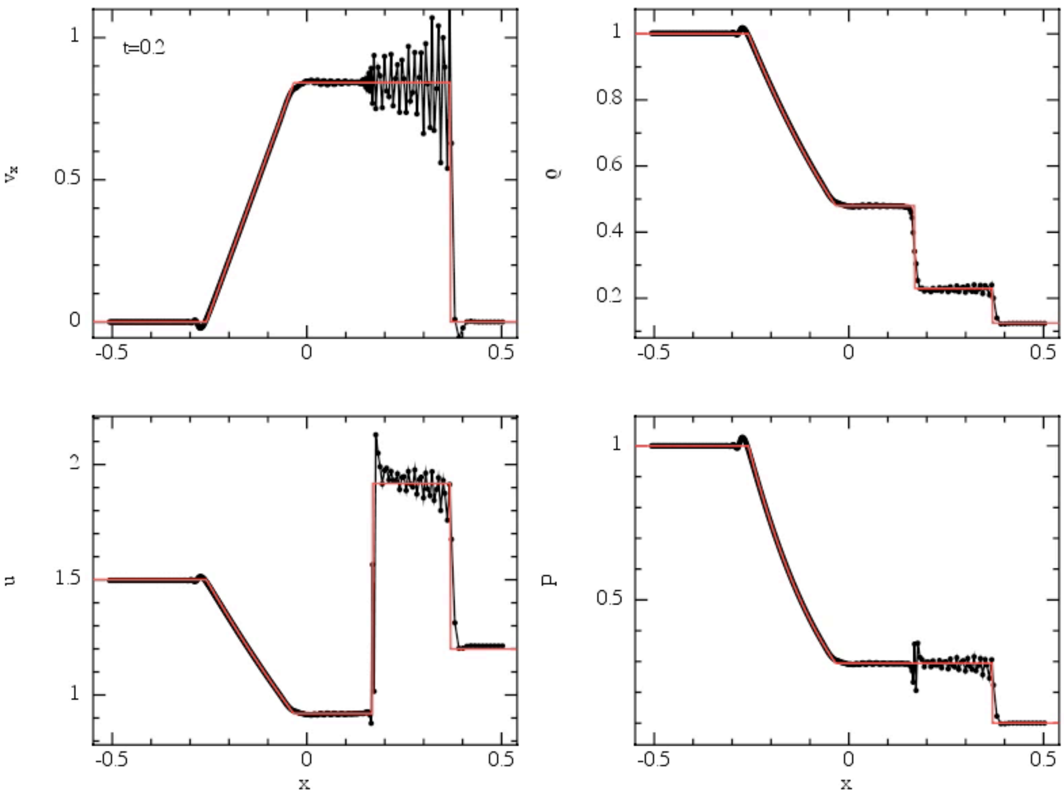

Zero dissipation... so we have to add some

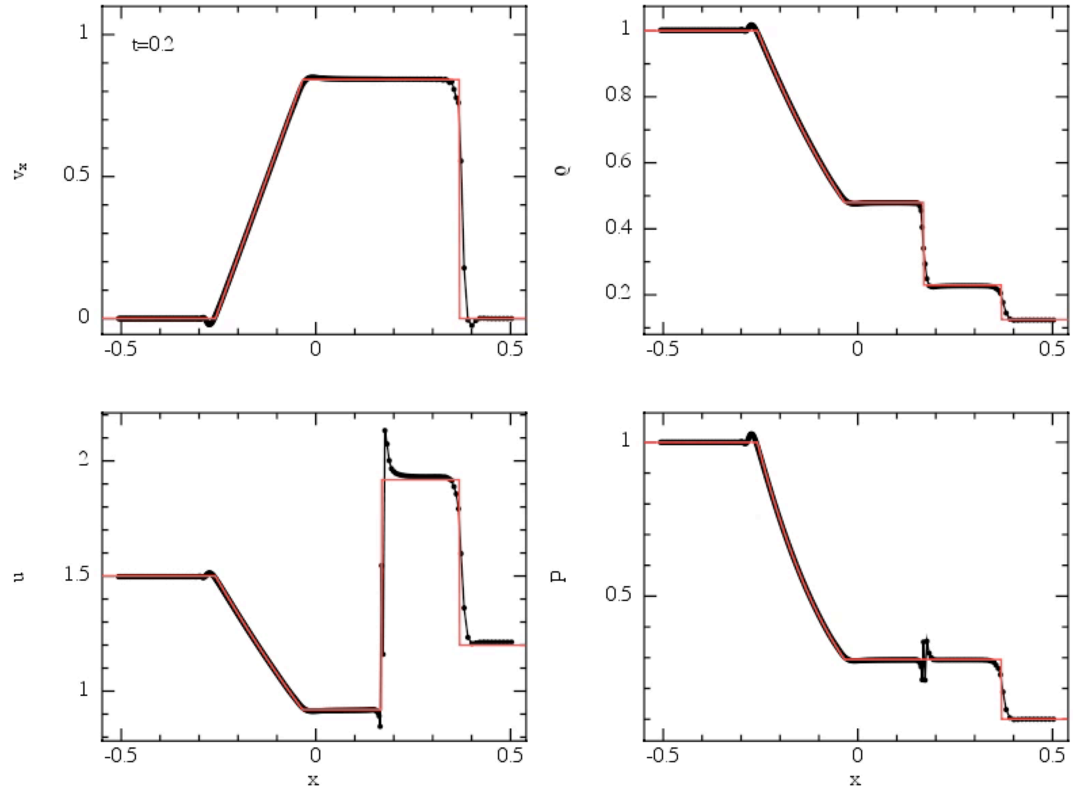

Must treat EVERY discontinuity

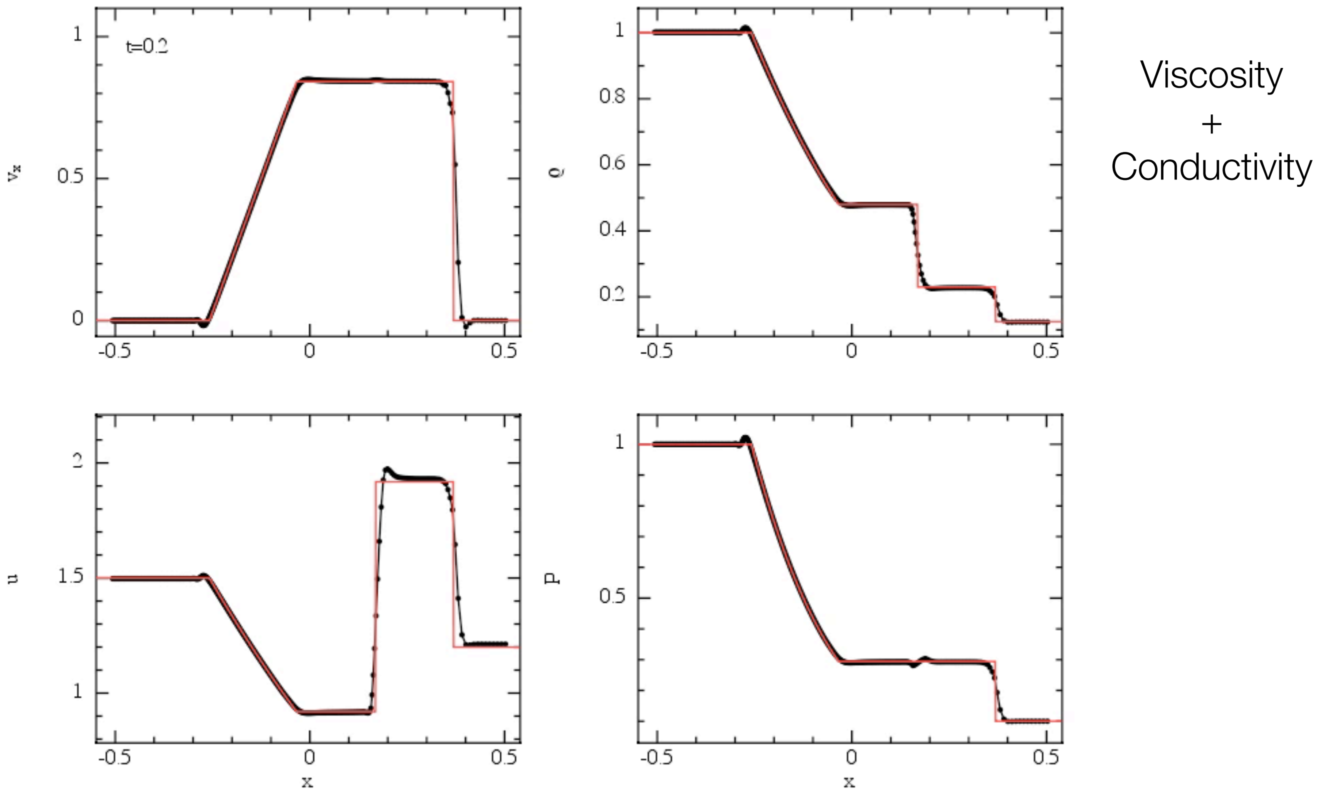

But must treat discontinuities properly...

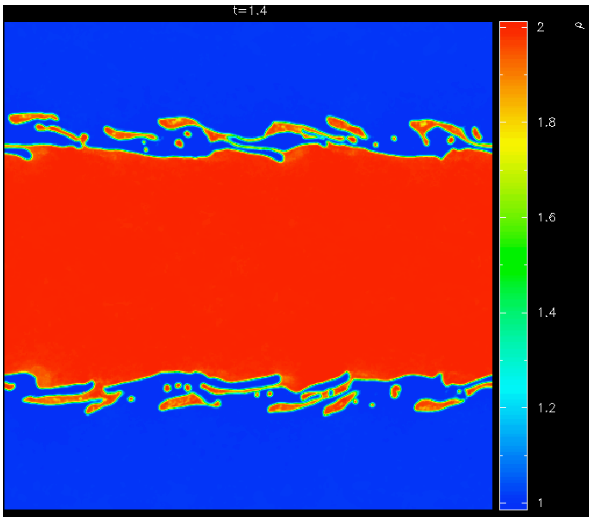

Viscosity only

This issue has NOTHING to do with the Kelvin-Helmholtz instability

Price (2008, J. Comp. Phys.)

Fundamental differences between SPH and grid methods

Oscar Agertz,[1★] Ben Moore,[1] Joachim Stadel,[1] Doug Potter,[1] Francesco Miniati,[2] Justin Read,[1] Lucio Mayer,[2] Artur Gawryszczak,[3] Andrey Kravtsov,[4] Åke Nordlund,[5] Frazer Pearce,[6] Vicent Quilis,[7] Douglas Rudd,[4] Volker Springel,[8] James Stone,[9] Elizabeth Tasker,[10] Romain Teyssier,[11] James Wadsley[12] and Rolf Walder[13]

[1] *Institute for Theoretical Physics, University of Zürich, CH-8057 Zürich, Swi*
[2] *Department of Physics, Institute für Astronomie, ETH Zürich, CH-8093 Z*
[3] *Nicolaus Copernicus Astronomical Centre, Bartycka 18, Warsaw PL-00-7*
[4] *Department of Astronomy & Astrophysics, The University of Chicago, Ch*
[5] *Niels Bohr Institute, Copenhagen University, Juliane Maries Vej 30, DK-2*
[6] *School of Physics and Astronomy, University of Nottingham, University P*
[7] *Departemento de Astronomia y Astrofisica, Universidad de Valencia, 461*
[8] *Max-Planck-Institute for Astrophysics, Karl-Schwarzschild-Str. 1, 85740*
[9] *Department of Astrophysical Sciences, Princeton University, Princeton, N*
[10] *Department of Astronomy, Columbia University, New York, NY 10027, U*
rophysique, CEA/DSM/DAPNIA/SAp, Centre d'Etudes de S
of Physics and Astronomy, McMaster University, Hamilton,
stronomie, ETH Zürich, CH-8092 Zürich, Switzerland

important dynamical instabilities such as Kelvin-Helmholtz or Rayleigh Taylor ... are poorly or not at all resolved by existing SPH techniques

...the reason for this is that SPH, at least in its standard implementation, introduces spurious pressure forces on particles in regions where there are steep density gradients

July 3. Received 2007 June 30; in original form 2006 October 16

ABSTRACT

We have carried out a comparison study of hydrodynamical codes by investigating their performance in modelling interacting multiphase fluids. The two commonly used techniques of grid and smoothed particle hydrodynamics (SPH) show striking differences in their ability to model processes that are fundamentally important across many areas of astrophysics. Whilst Eulerian grid based methods are able to resolve and treat important dynamical instabilities, such as Kelvin–Helmholtz or Rayleigh–Taylor, these processes are poorly or not at all resolved by existing SPH techniques. We show that the reason for this is that SPH, at least in its standard implementation, introduces spurious pressure forces on particles in regions where there are steep density gradients. This results in a boundary gap of the size of an SPH smoothing kernel radius over which interactions are severely damped.

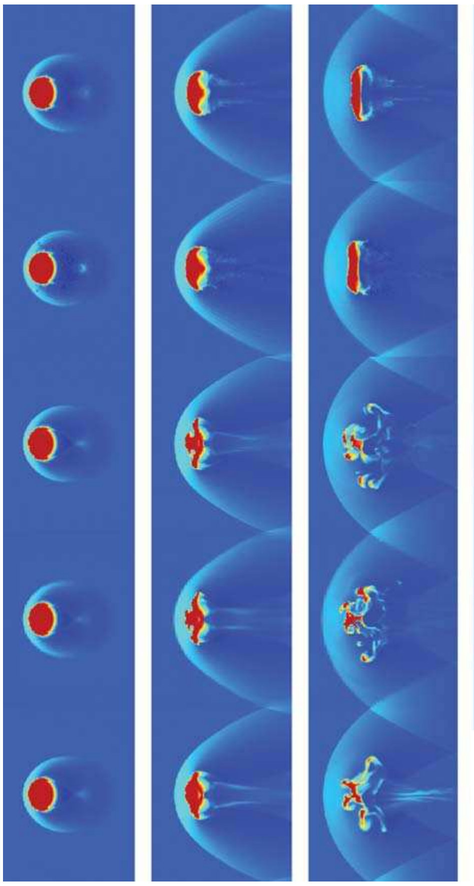

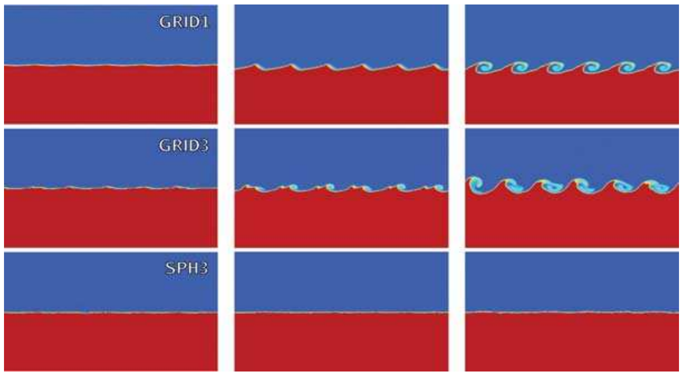

Figure 13. Density slices of, from top to bottom, GRID1, GRID3 and SPH3. The panels show the KH simulation at $t = \tau_{KH}/3$, $2\tau_{KH}/3$ and τ_{KH}. ′ simulations show clear growth of the KHI while this is completely absent in SPH.

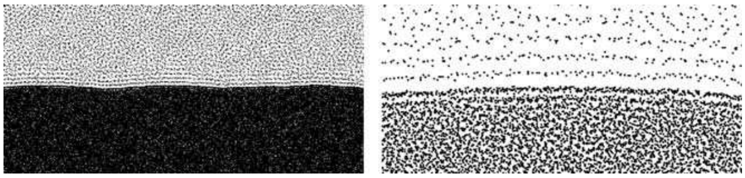

Figure 14. A close up view of the SPH particles at the boundaries between the shearing layers (left) and closer zoom in (right) for SPH3 at τ_{KH}. We ca see empty layers formed through erroneous pressure forces due to improper density calculations at density gradients. Even though the two fluids are relative to each other, the gap is so large that proper fluid interaction is severely decreased or even absent.

Figure 15. A zoom in of the SPH particles at the boundaries between the shearing layers for the isodensity SPH run with standard viscosity (left) and low viscosity (right) at τ_{KH}. The black and white regions are particles that belonged to the initially separated shearing layers. We clearly see growth of the KHI in the standard implementation of SPH, and even stronger for the low viscosity version. The simulation was performed with GASOLINE using 10^6 particles in the same way as SPH3 described in Section 6.2.

nsity slices through the centre of the cloud at $t = 0.25$, 1.0, 1.75 and 2.5 τ_{KH}. From top (ENZO_256), FLASH (FLASH_256) and ART-HYDRO (ART_256). The grid simulations clearly s H, unlike the SPH simulations in which most of the gas remains in a single cold dense blob.

Must treat EVERY discontinuity

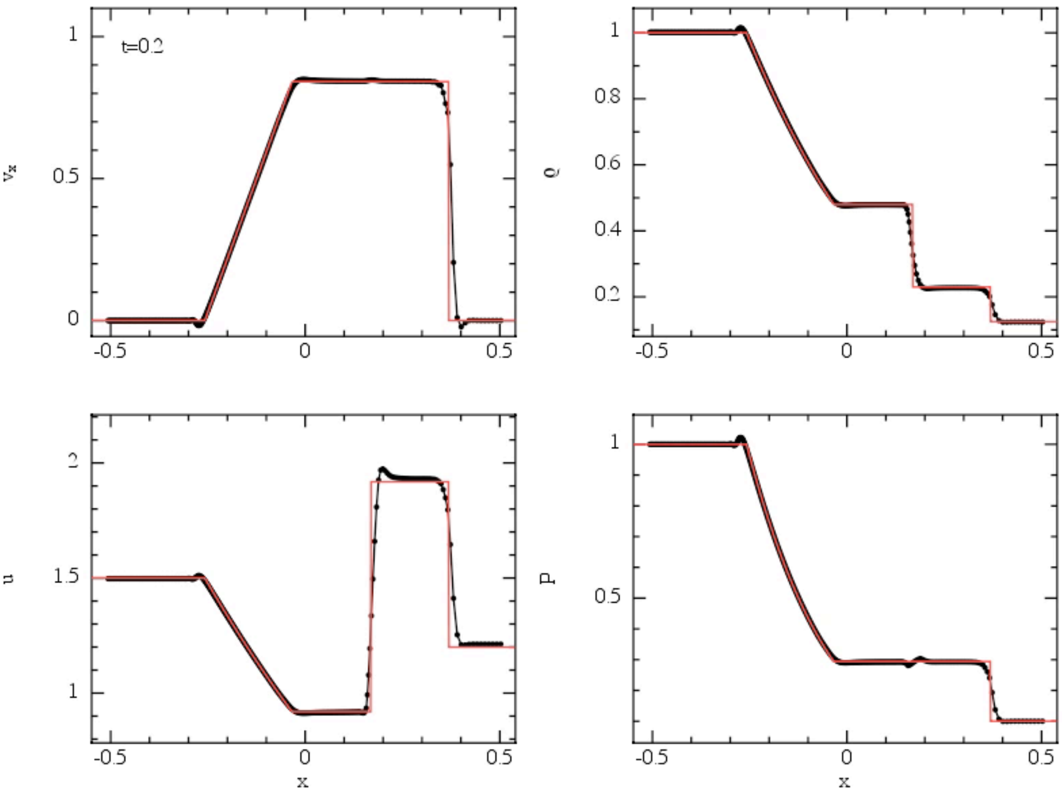

Viscosity
+
Conductivity

But must treat discontinuities properly...

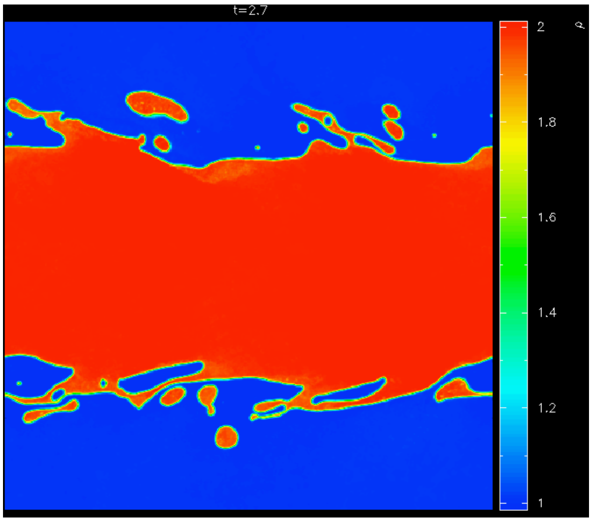

Viscosity only

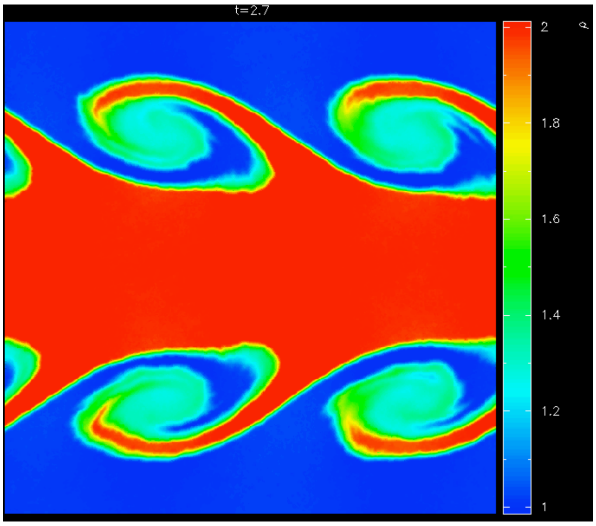

Viscosity + conductivity

This issue has NOTHING to do with the Kelvin-Helmholtz instability

Price (2008, J. Comp. Phys.)

Richtmyer-Meshkov Instability

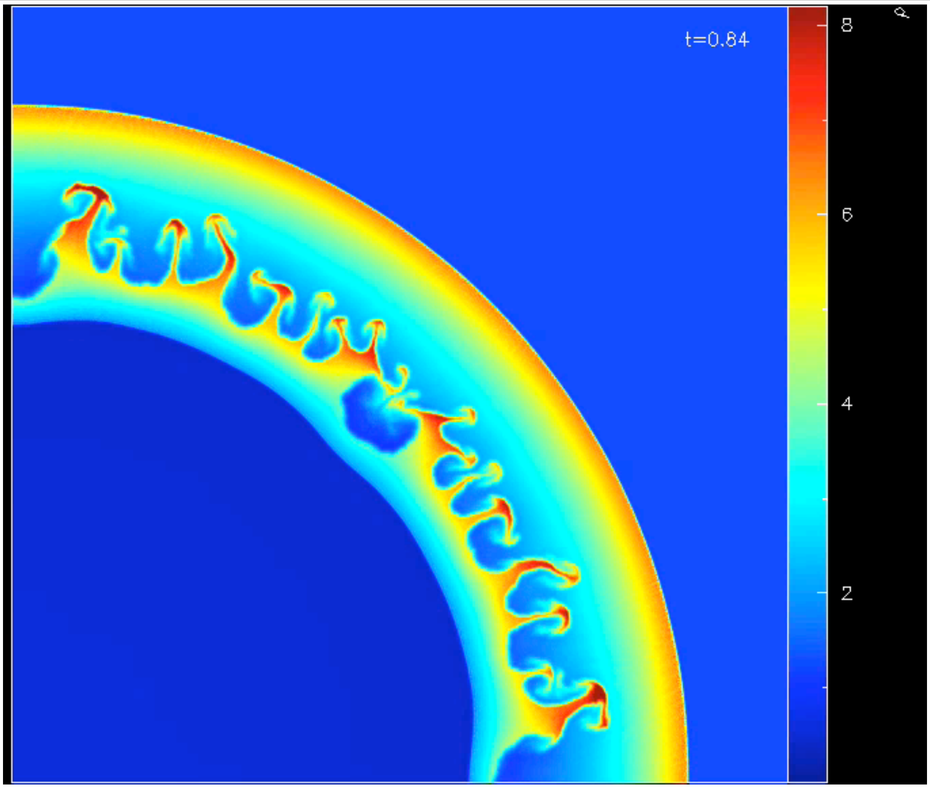

Exploding blob (Børve & Price 2010)

dissipation terms need to be explicitly added

The key is a good switch

6 *Lee Cullen & Walter Dehnen*

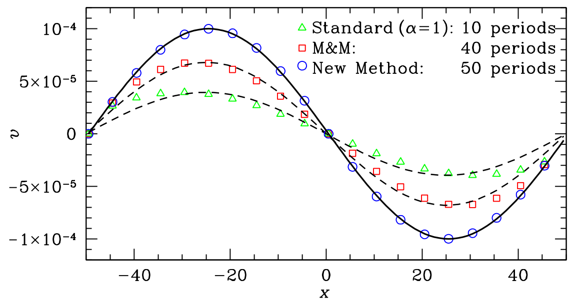

Figure 2. As Fig. 1, but for SPH with standard ($\alpha = 1$) or Morris & Monaghan (1997) artificial viscosity, as well as our new method (only every fifth particle is plotted). Also shown are the undamped wave (*solid*) and lower-amplitude sinusoidals (*dashed*). Only with our method the wave propagates undamped, very much like SPH without any viscosity, as in Fig. 1.

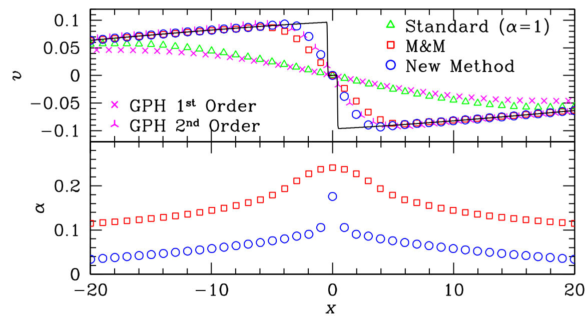

Figure 6. Steepening of a 1D sound wave: velocity and viscosity parameter vs. position for standard SPH, the M&M method, our new scheme, and Godunov particle hydrodynamics of first and second order (GPH, Cha & Whitworth 2003), each using 100 particles per wavelength. The solid curve in the top panel is the solution obtained with a high-resolution grid code.

Cullen & Dehnen (2010), see also Read & Heyfield (2011)

Use of these switches removes the main disadvantage of SPH as used in numerical cosmology

Exact conservation

Exact conservation: Advantages

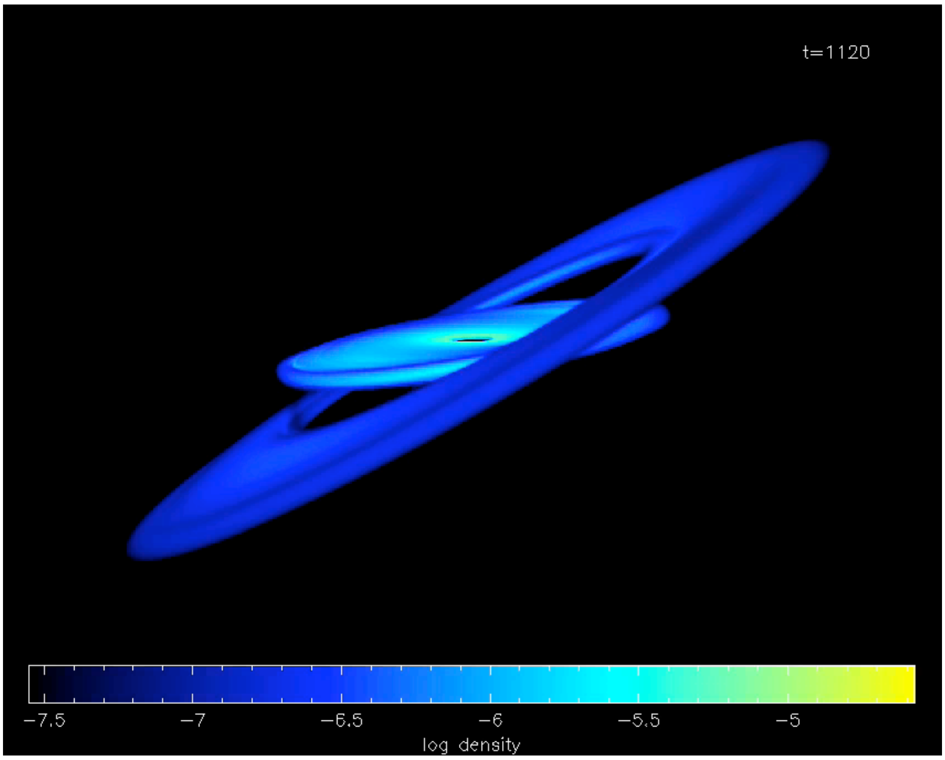

Lodato & Price (2010)

Orbits are orbits... even when they're not aligned with any symmetry axis.

Exact conservation: Disadvantages

- Calculations keep going, even when they're screwed up...

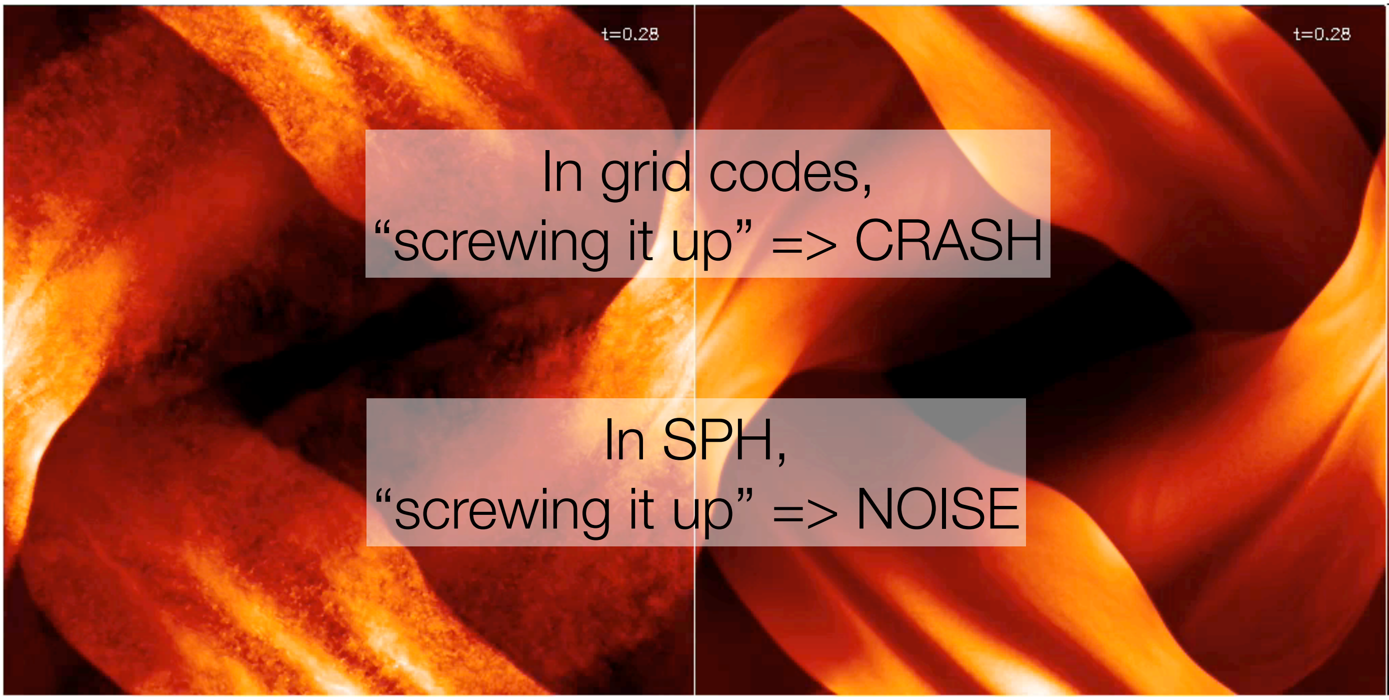

Orszag-Tang Vortex in MHD (c.f. Price & Monaghan 2005, Rosswog & Price 2007, Price 2010)

2D Orszag-Tang Vortex: Energy conservation

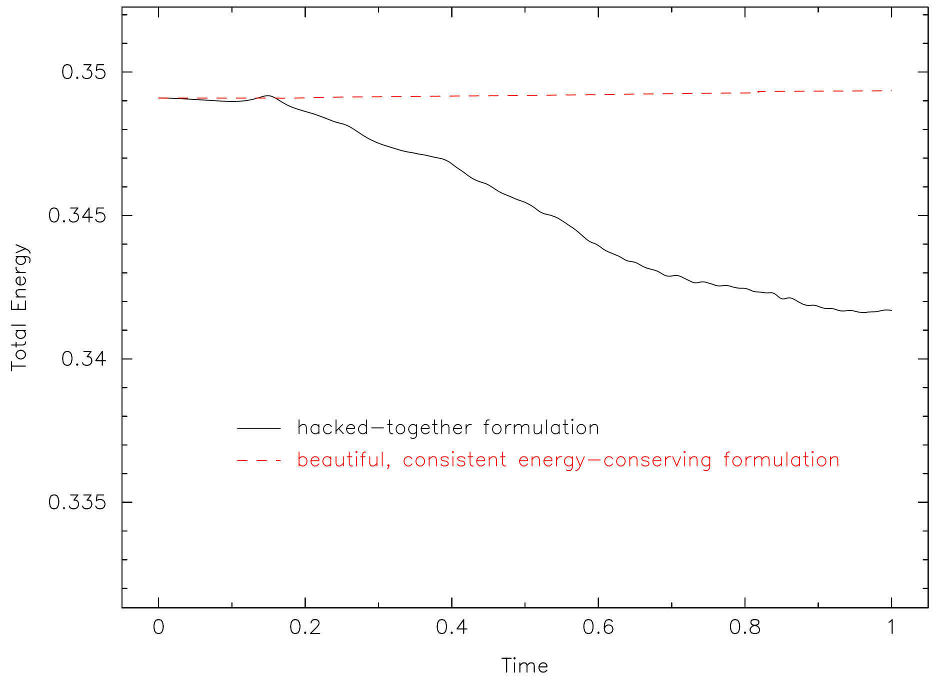

What this gives us: Advantages of SPH

- An exact solution to the continuity equation
- Resolution follows mass
- ZERO dissipation
- Advection done perfectly
- EXACT conservation of mass, momentum, angular momentum, energy and entropy
- A guaranteed minimum energy state

The minimum energy state

The “grid” in SPH...

What happens to a random particle arrangement?

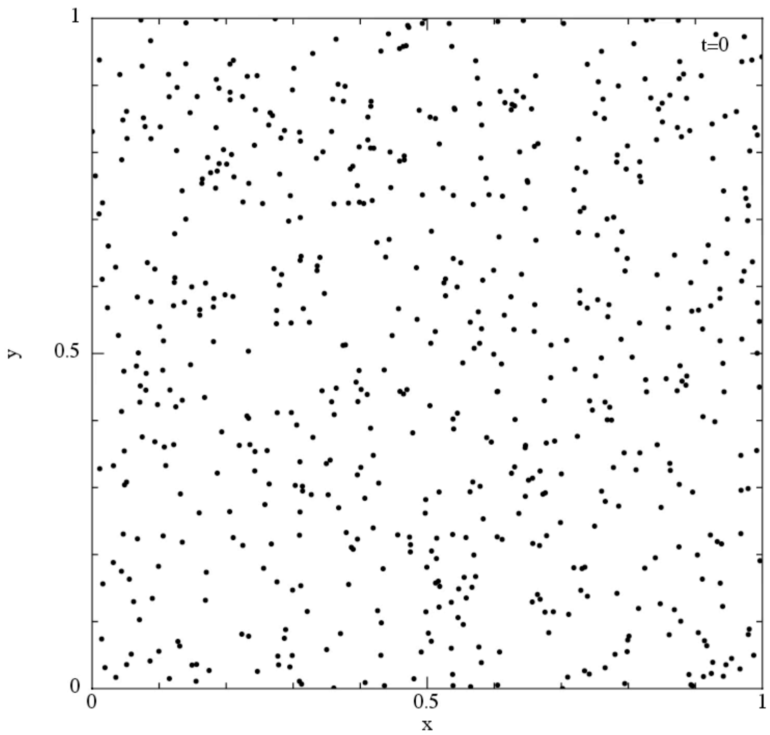

$$\frac{\mathrm{d}\mathbf{v}_i}{\mathrm{d}t} = -\sum_j m_j \left(\frac{P_i}{\rho_i^2} + \frac{P_j}{\rho_j^2}\right) \nabla_i W_{ij}$$

SPH particles know how to stay regular

Why “rpSPH” (Morris 1996, Abel 2010) is a bad idea

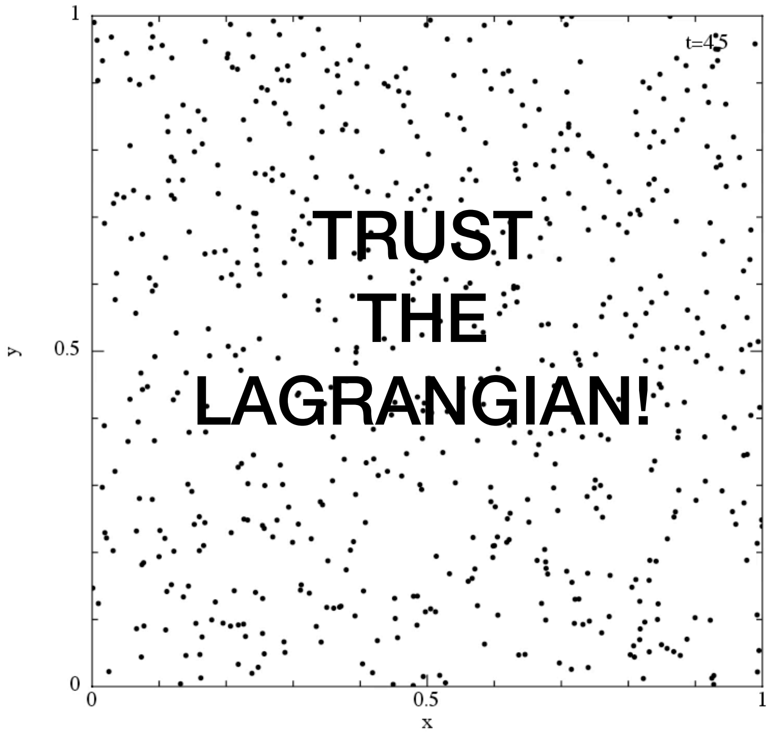

$$\frac{\mathrm{d}\mathbf{v}_i}{\mathrm{d}t} = \sum_j m_j \left(\frac{P_i - P_j}{\rho_j^2} \right) \nabla_i W_{ij}$$

Improving the gradient operator leads to WORSE results

Corollary: Better to use a worse but conservative gradient operator

Corollary: Need positive pressures

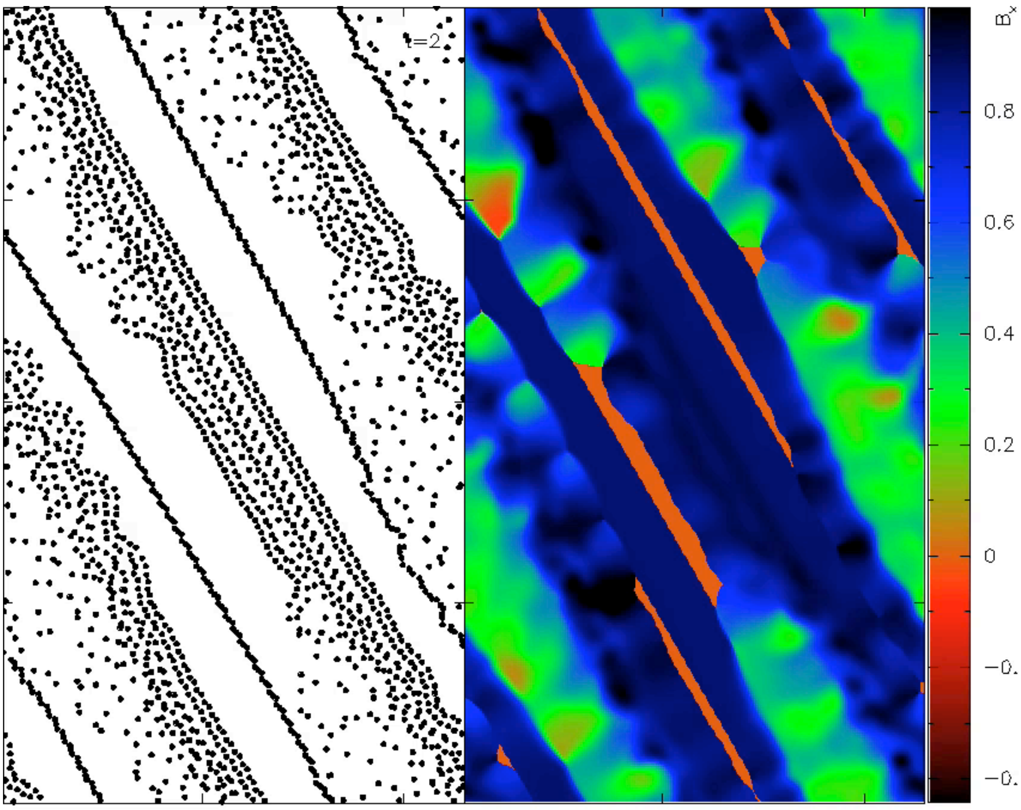

Compromise approach gives stability

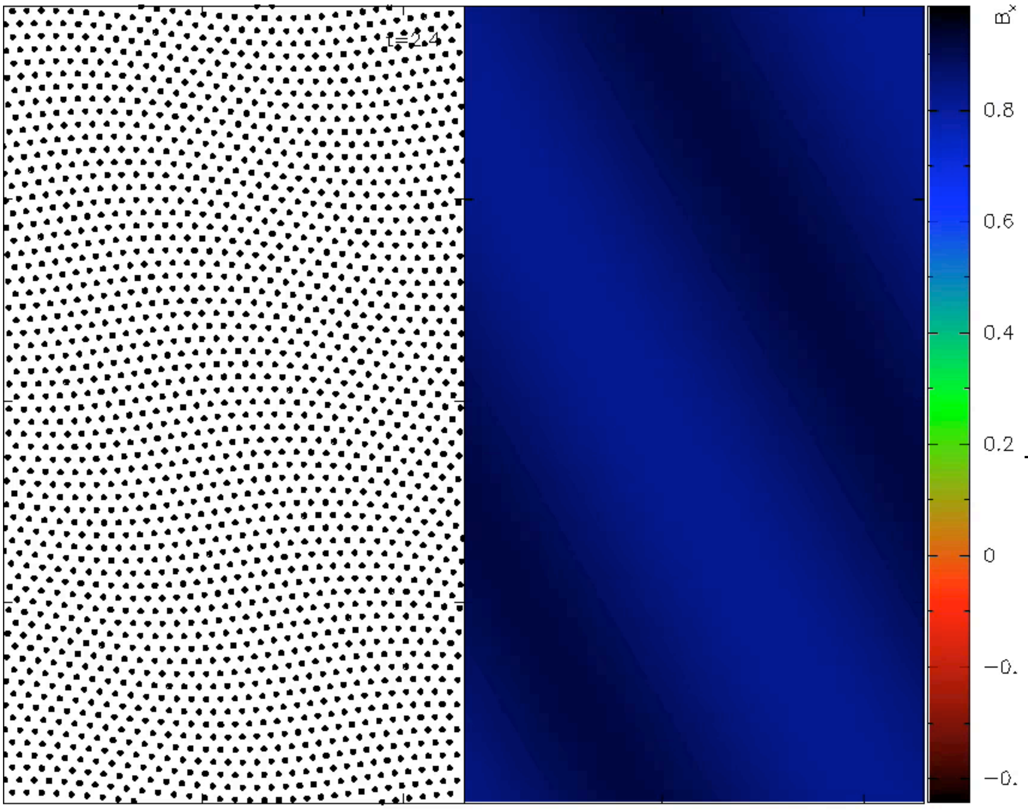

Subtract

$$-\mathbf{B}(\nabla \cdot \mathbf{B})$$

from MHD force:

Stable but nonconservative

2D shock tube

- intrinsic “remeshing” of particles

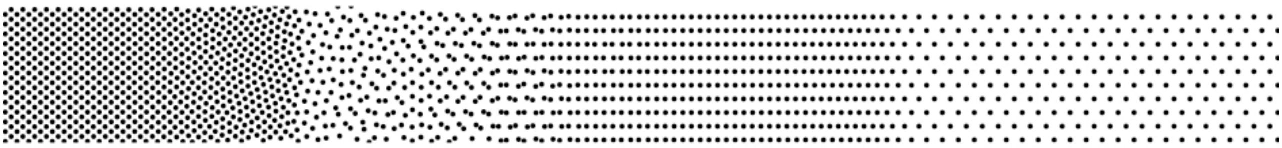

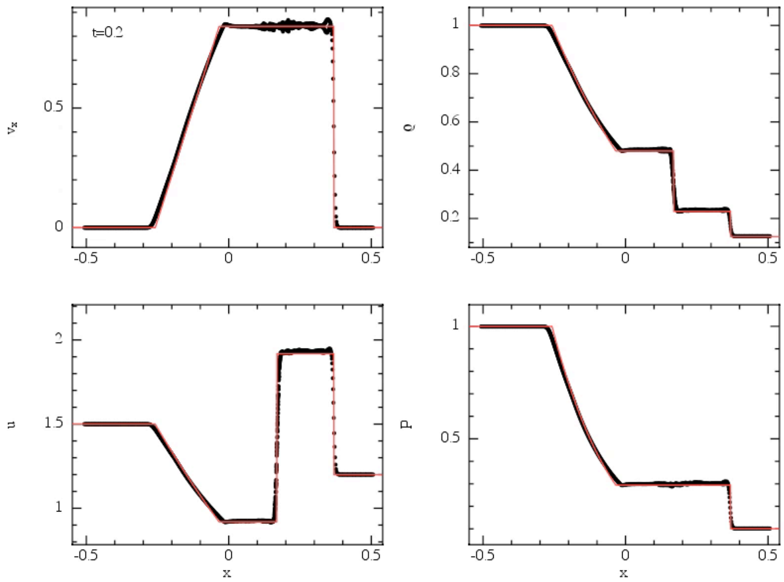

Why you cannot use “more neighbours” (or: How to halve your resolution)

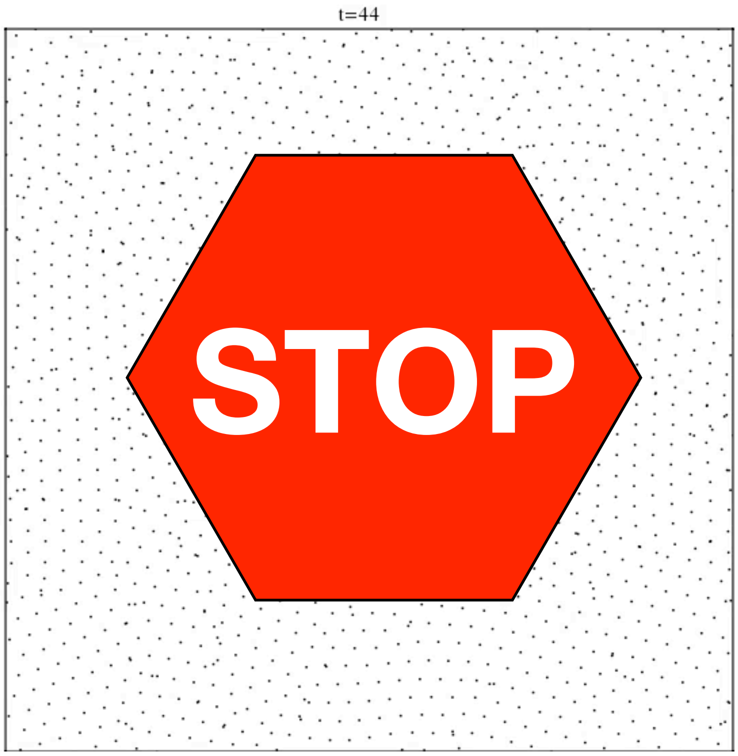

pairing occurs for > 65 neighbours for the cubic spline in 3D

N_{neigh} should NOT be a free parameter!

i.e., should not change the ratio of smoothing length to particle spacing

2D shock tube

- use smoother quintic kernel - truncated at 3h instead of 2h (NOT the same as “more neighbours” with the cubic spline)

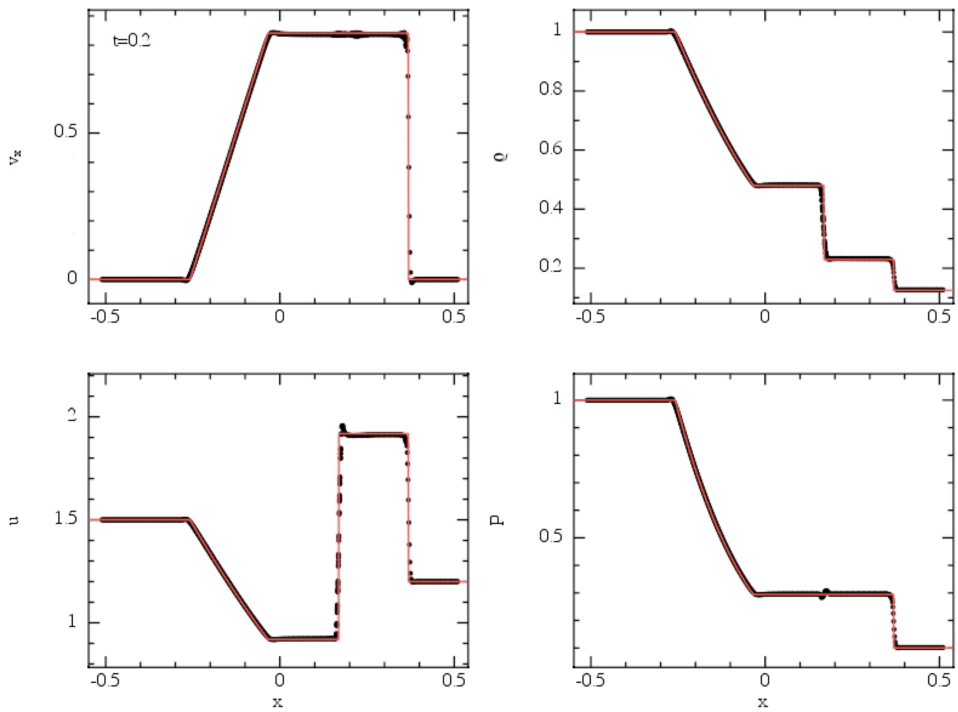

Grid vs. SPH: Turbulence

Price & Federrath (2010): Comparison of driven, supersonic, isothermal turbulence

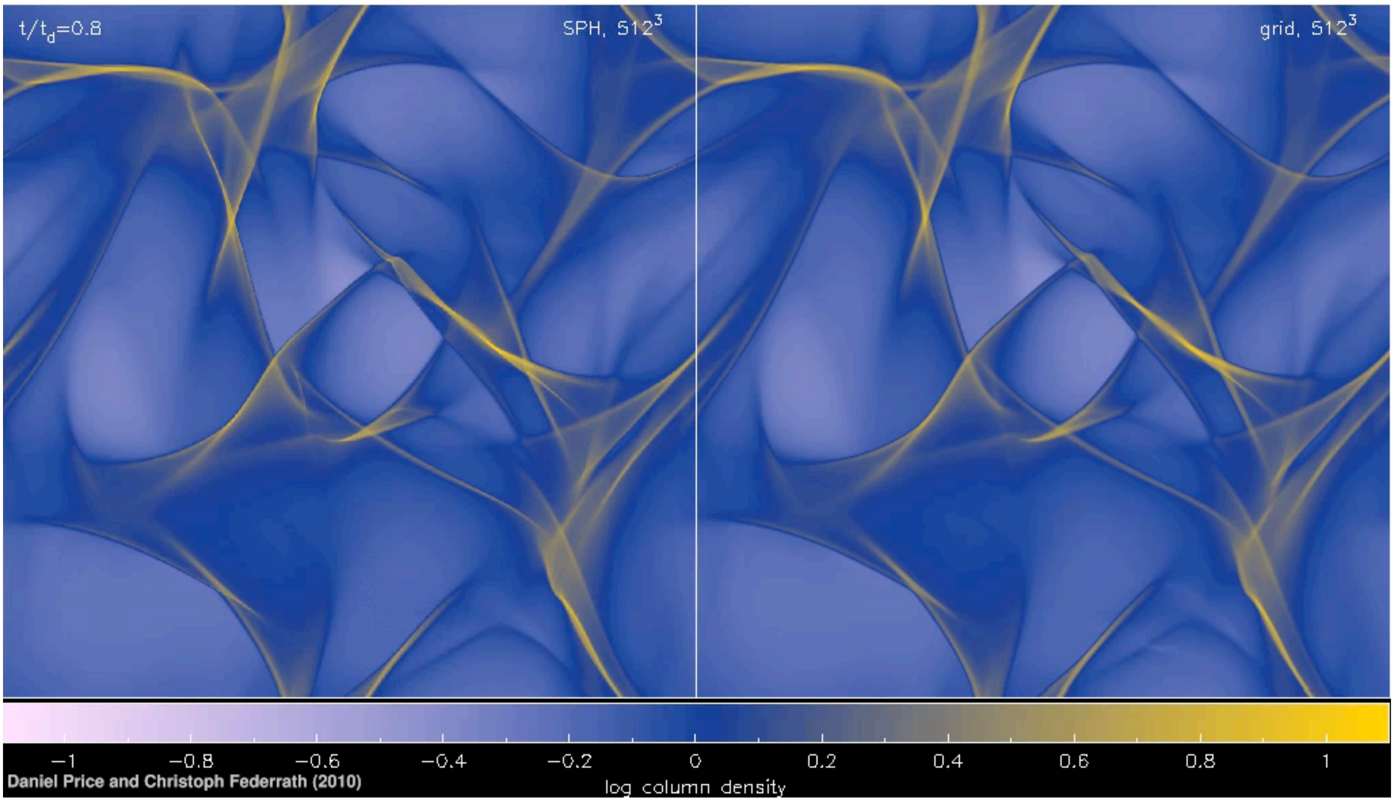

PHANTOM

FLASH

Mach 10

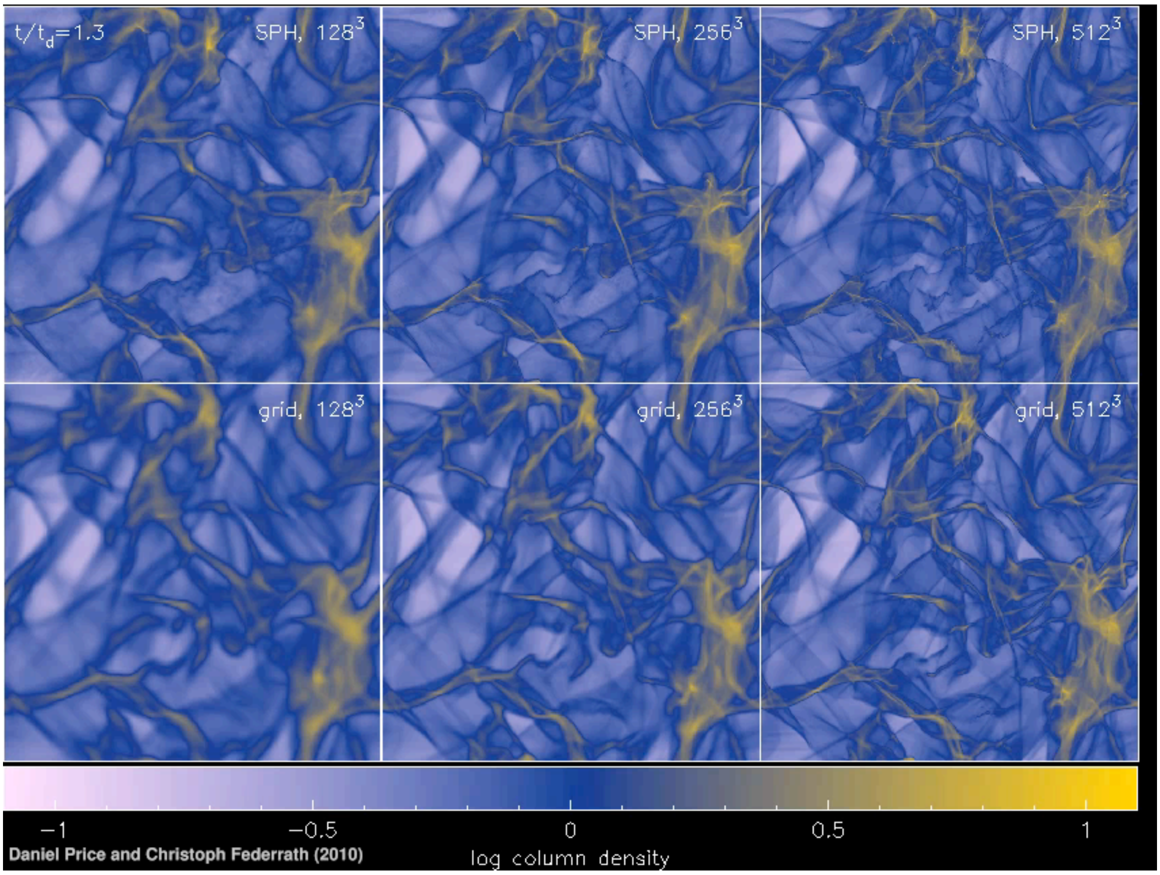
t/t_d=1.3
SPH, 128^3
SPH, 256^3
SPH, 512^3
grid, 128^3
grid, 256^3
grid, 512^3
−1
−0.5
0
0.5
1
Daniel Price and Christoph Federrath (2010)
log column density

Slice:

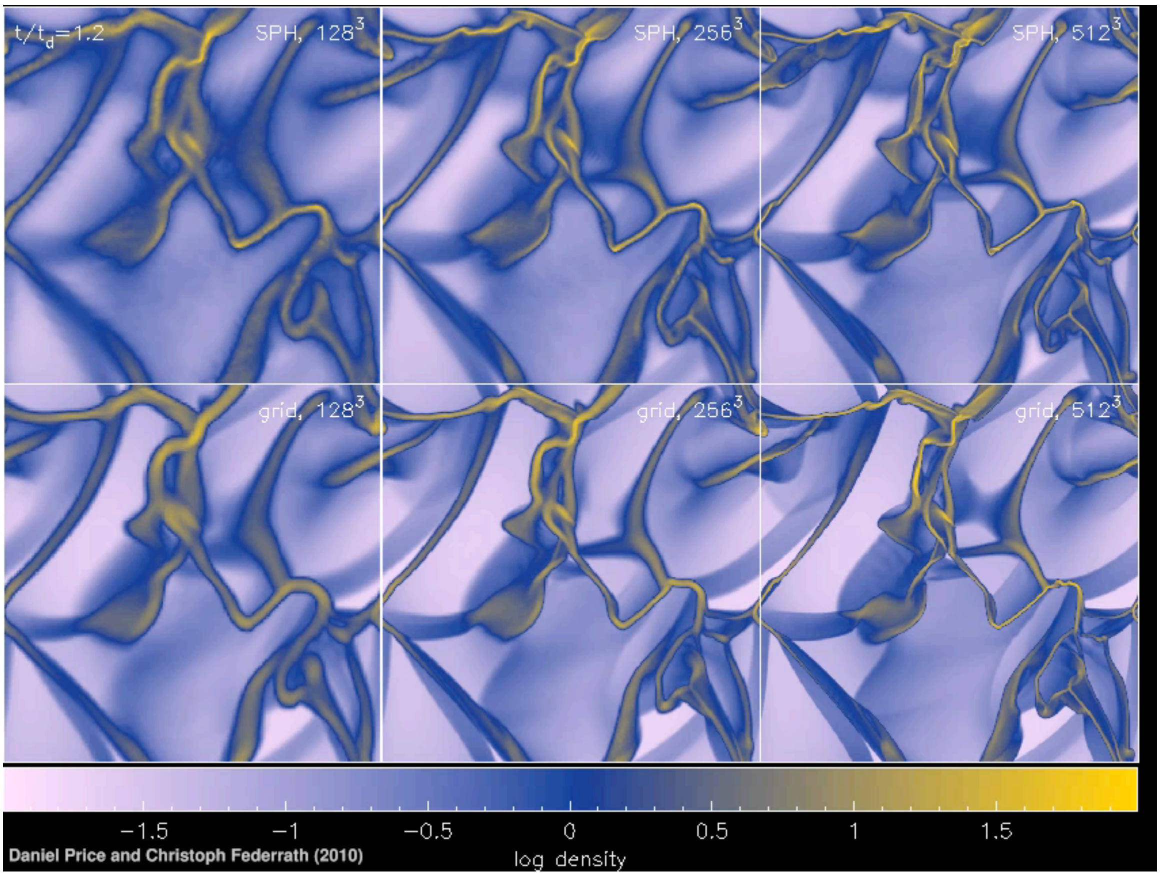
t/t_d=1.2
SPH, 128^3
SPH, 256^3
SPH, 512^3
grid, 128^3
grid, 256^3
grid, 512^3
−1.5
−1
−0.5
0
0.5
1
1.5
Daniel Price and Christoph Federrath (2010)
log density

Kinetic energy spectra (time averaged)

Burgers-like k^{-2} spectrum in the kinetic energy for Mach 10 hydro

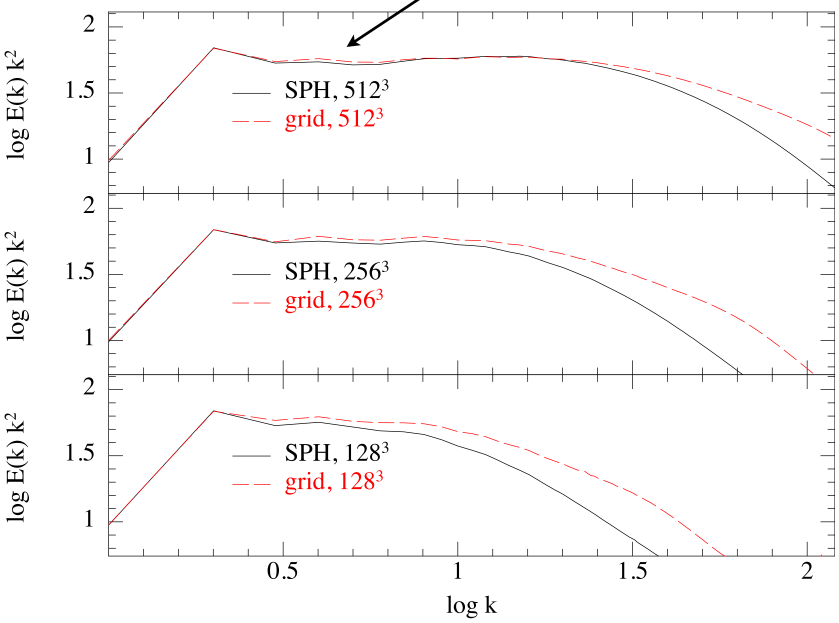

Price & Federrath (2010)

Density-weighted energy spectra $(\rho^{1/3}\mathbf{v})$

Confirms Kritsuk et al. (2007) suggestion of Kolmogorov-like $k^{-5/3}$ spectrum in this variable

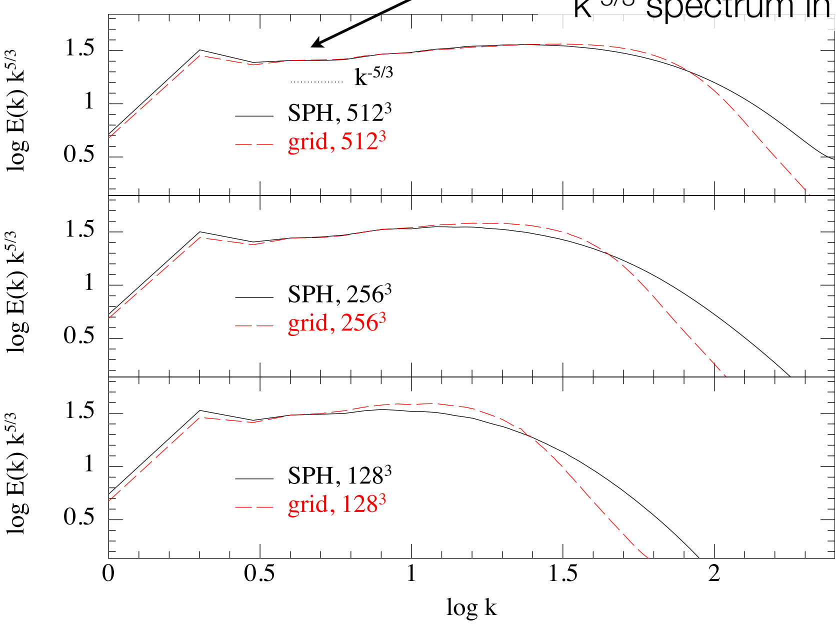

Price & Federrath (2010)

But SPH resolution is in density field

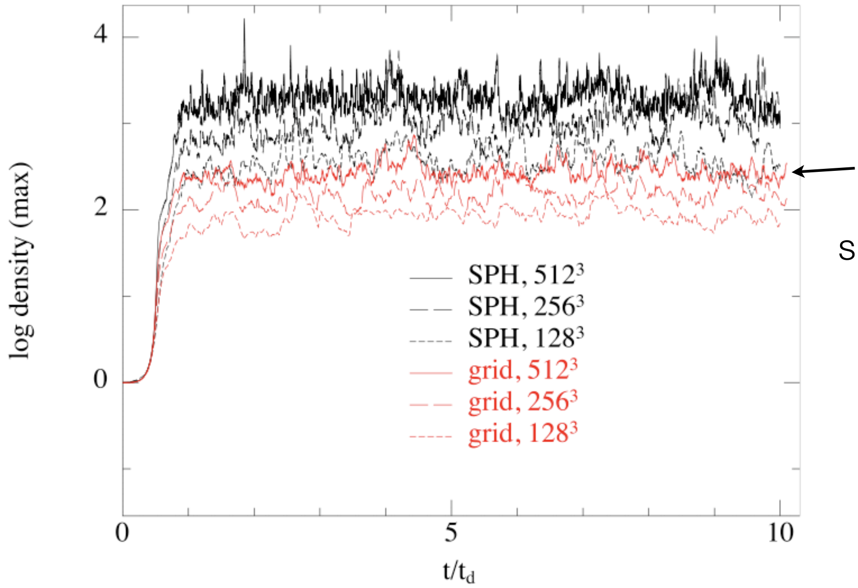

max density in SPH at 128^3 similar to max grid density at 512^3

Price & Federrath (2010)

Density PDFs:

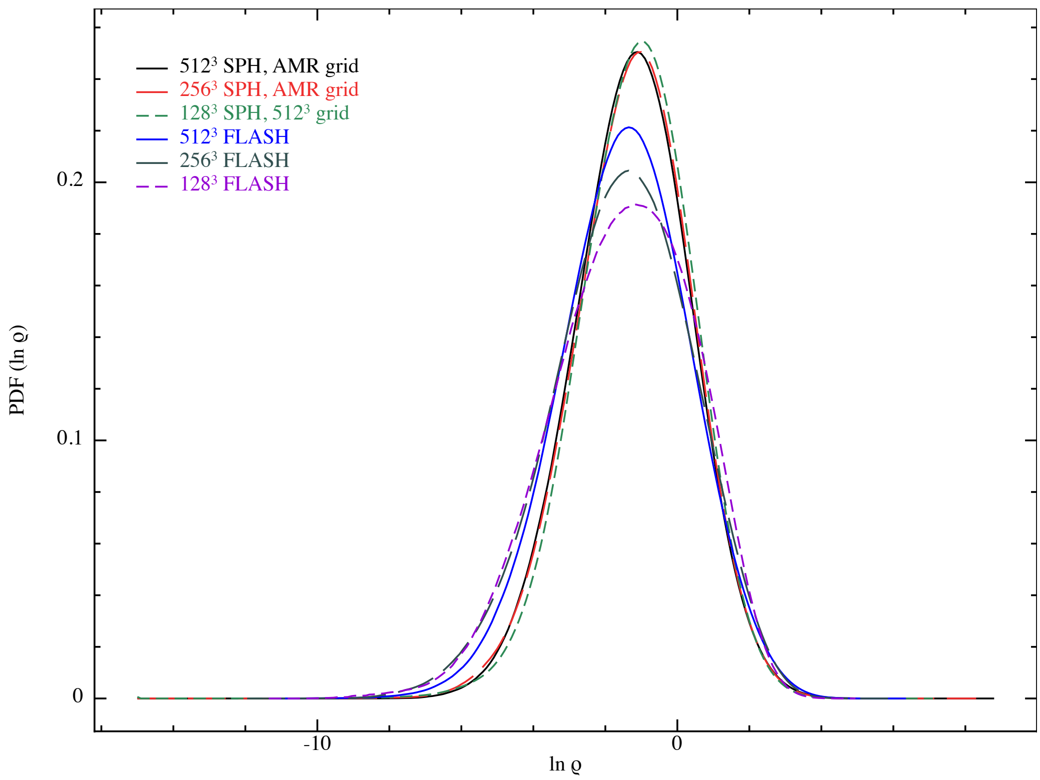

What about low Mach number turbulence?

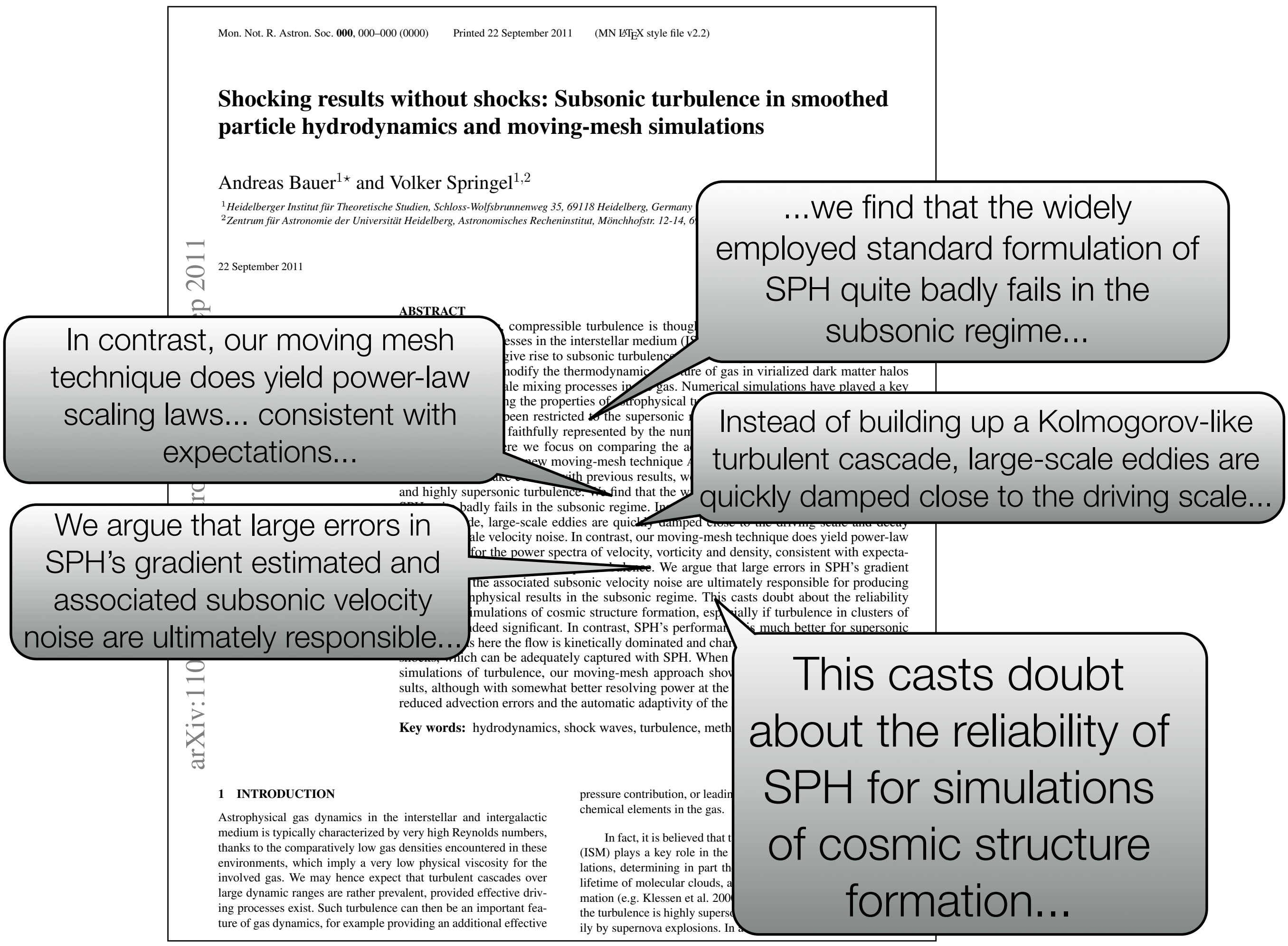

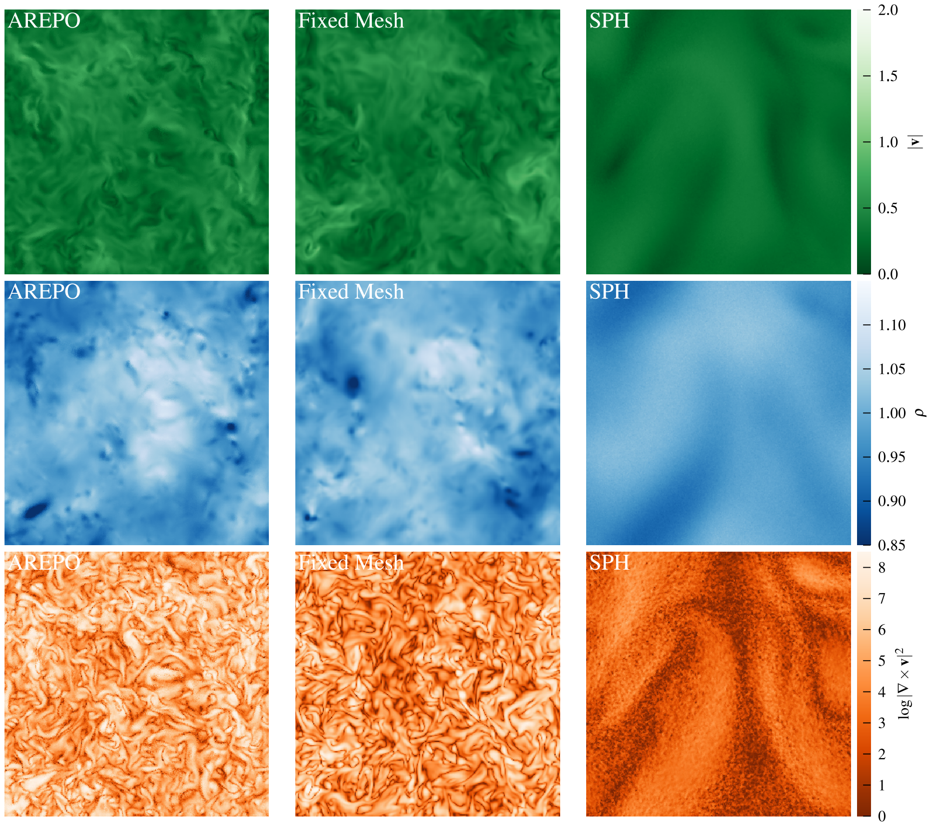

Figure 3. Visual comparison of the turbulent velocity field (top row), the density field (middle row) and the enstrophy $|\nabla \times \boldsymbol{v}|^2$ (bottom row) in quasi-stationary turbulence with $\mathcal{M} \sim 0.3$, simulated with different numerical techniques. Shown are thin slices through the middle of the perdiodic simulation box. From left to right, we show our moving grid result, an equivalent calculation on a static mesh, and an SPH calculation, as labeled.

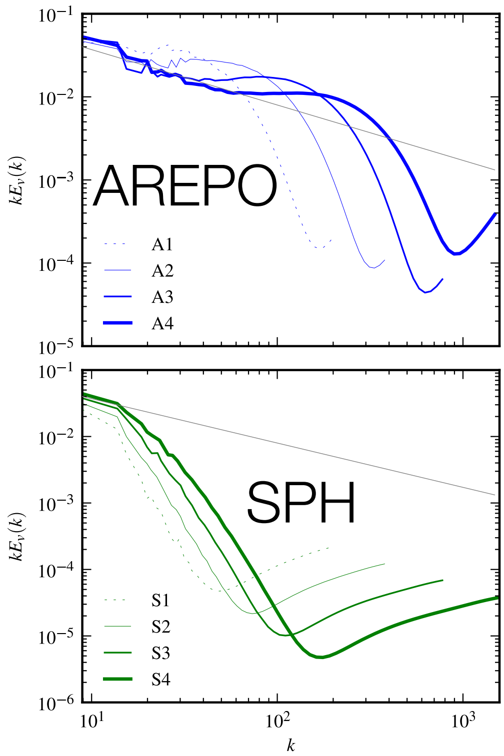

What's going on?

Figure 5. Convergence study for the velocity power spectrum of $\mathcal{M} \sim 0.3$ subsonic turbulence. The panel on top shows results for AREPO, from a resolution of 64^3 to 512^3 cells. The panel on the bottom gives the corresponding results for SPH. However, even at a high resolution as high 512^3 particles, no extended inertial range of turbulence can be identified in SPH. The thin grey lines show the power-law expected for Kolmogorov's theory.

BS explanation:

We argue that the origin of this noise lies in errors of SPH's gradient estimate. Numerous studies have pointed out that the standard approach followed in SPH for constructing derivatives of smoothed fluid quantities involves rather large error terms, especially for the comparatively irregular particle distributions in multi-dimensional simulations. The problem lies in a lack of consistency of the ordinary density estimates (which do not conserve volume, i.e. the sum of m_i/ρ_i is not guaranteed to add up to the total volume) and in a low order of the gradient estimate itself (e.g. Quinlan et al. 2006; Gaburov & Nitadori 2011; Amicarelli et al. 2011). In practice, this means that there can be pressure forces on particles even though all individual pressure values of the particles are equal,

A clue:

port. To suppress the artificial viscosity in regions of strong shear, Balsara (1995) proposed a simple viscosity limiter in the form of an additional multiplicative factor $(f_i + f_j)/2$ for the viscous tensor, defined as

$$f_i = \frac{|\nabla \cdot \boldsymbol{v}|_i}{|\nabla \cdot \boldsymbol{v}|_i + |\nabla \times \boldsymbol{v}|_i}. \tag{3}$$

This limiter is often used in cosmological SPH simulations and also available in the GADGET code. In our default simulations, we have refrained from enabling it, but we have also run comparison simulations where it is used, as discussed in our results section.

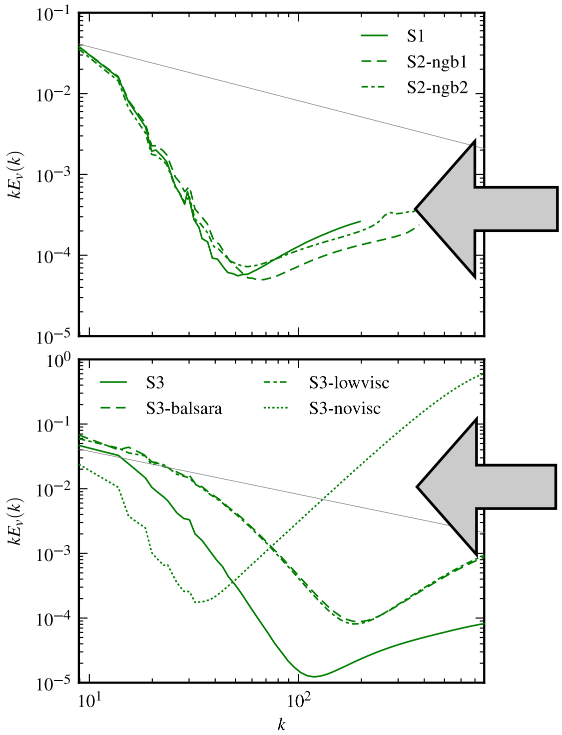

effect of “gradient error”
(neighbour number)

effect of viscosity

Figure 7. Dependence of SPH turbulence results on numerical nuisance parameters. The panel on top gives results for the velocity power spectrum when the number of SPH smoothing neighbours is increased, from our default of 64 to 180, and finally to 512. Formally, the later run with 128^3 particles has the same mass and spatial resolution as our S1 run with 64^3 particles, hence the latter is included as a dashed line. The bottom panel illustrates the effect of changing the SPH viscosity parameterization. For lower α, the velocity power on large scales goes up, but the shape of the power spectrum does not improve. Note however that this also increases the

But what is the Reynolds number?

$$\mathcal{R}_e \equiv \frac{VL}{\nu}$$

Stokes (1851), Reynolds (1883)

Dissipation in SPH

There is none (it is a Hamiltonian system)
...except what you explicitly add.

AV terms give:

$$\nu \approx \frac{1}{10}\alpha v_{\rm sig} h; \qquad \zeta \approx \frac{1}{6}\alpha v_{\rm sig} h$$

Monaghan & Lattanzio (1985): $\alpha = 1$

Morris & Monaghan (1997): $\alpha(x, t) \in [0.1, 1]$

Reynolds numbers in SPH

$$\mathcal{R}_{\rm e} = \frac{10}{\alpha}\mathcal{M}\frac{L}{h},$$

Price & Federrath (2010), Mach 10:

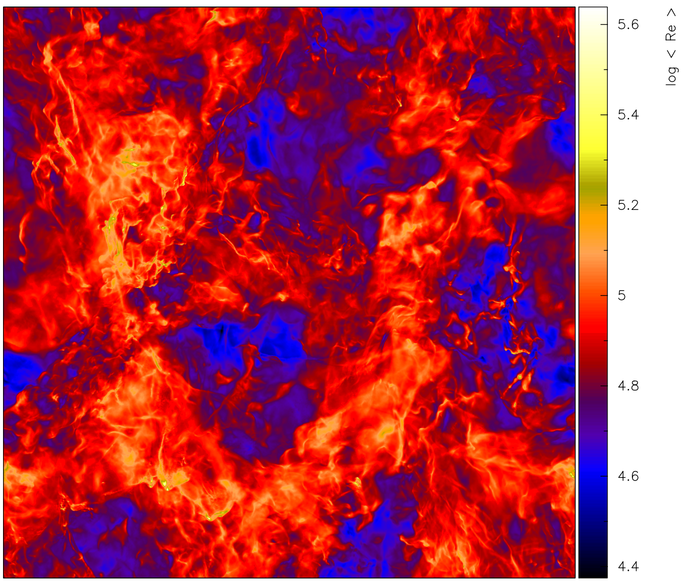

c.f. Elmegreen & Scalo (2004): $R_e \sim 10^5$-10^7 in ISM

Reynolds numbers in SPH

$$\mathcal{R}_{\rm e} = \frac{10}{\alpha}\mathcal{M}\frac{L}{h},$$

Linear dependence on Mach number

$$\mathcal{R}_{\rm e} = 2.4 n^{1/3} \left(\frac{\mathcal{M}}{0.3}\right)\left(\frac{\alpha}{1.0}\right)^{-1}\left(\frac{N_{\rm ngb}}{64}\right)^{-1/3},$$

In BS calculations:

$n = 64^3$	$n = 128^3$	$n = 256^3$
$\mathcal{R}_{\rm e} = 154$	$\mathcal{R}_{\rm e} = 307$	$\mathcal{R}_{\rm e} = 614$

Using standard (15yo) viscosity switches:

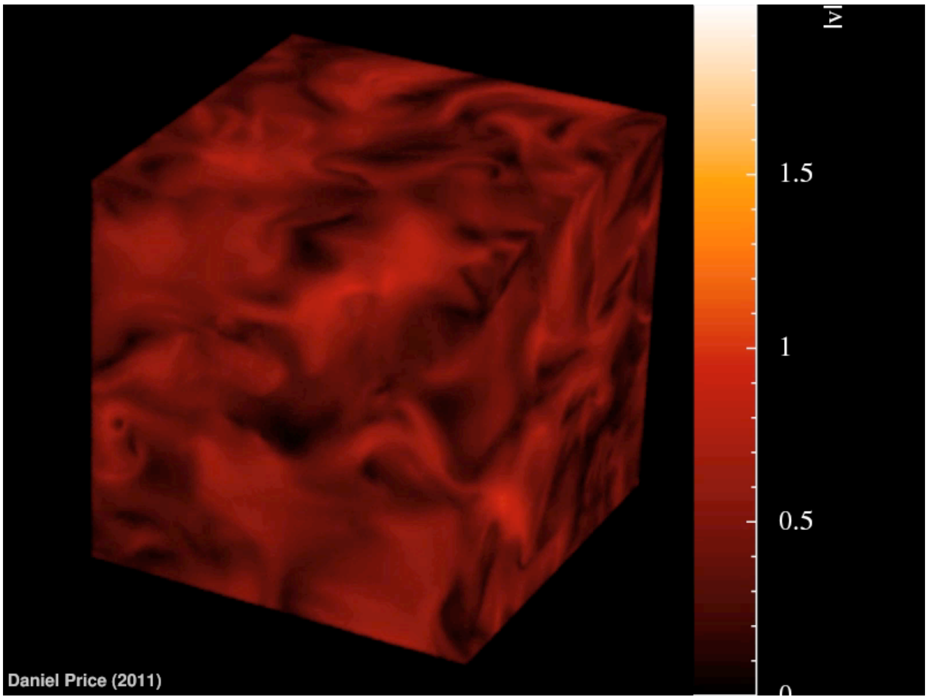

see also Dolag et al. (2005) and Valdarnini (2011) on importance of viscosity switches for SPH simulations of ICM/IGM turbulence

Also, much better viscosity switches now available (e.g. Cullen & Dehnen 2010)

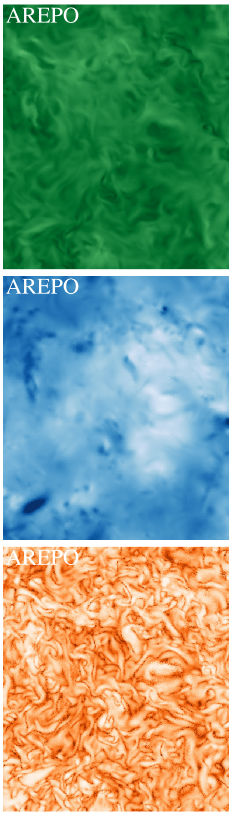

Figure 3. Visual comparison of the turbul
turbulence with $\mathcal{M} \sim 0.3$, simulated wit
to right, we show our moving grid result,

Monthly Notices of the ROYAL ASTRONOMICAL SOCIETY LETTERS

Mon. Not. R. Astron. Soc. **420,** L33–L37 (2012) doi:10.1111/j.1745-3933.2011.01187.x

Resolving high Reynolds numbers in smoothed particle hydrodynamics simulations of subsonic turbulence

Daniel J. Price⋆

Monash Centre for Astrophysics (MoCA) and School of Mathematical Sciences, Monash University, VIC 3800, Australia

Accepted 2011 November 4. Received 2011 November 4; in original form 2011 October 24

ABSTRACT

Accounting for the Reynolds number is critical in numerical simulations of turbulence, particularly for subsonic flow. For smoothed particle hydrodynamics (SPH) with constant artificial viscosity coefficient α, it is shown that the effective Reynolds number in the absence of explicit physical viscosity terms scales linearly with the Mach number – compared to mesh schemes, where the effective Reynolds number is largely independent of the flow velocity. As a result, SPH simulations with $\alpha = 1$ will have low Reynolds numbers in the subsonic regime compared to mesh codes, which may be insufficient to resolve turbulent flow. This explains the failure of Bauer & Springel to find agreement between the moving-mesh code AREPO and the GADGET SPH code on simulations of driven, subsonic ($v \sim 0.3c_s$) turbulence appropriate to the intergalactic/intracluster medium, where it was alleged that SPH is somehow fundamentally incapable of producing a Kolmogorov-like turbulent cascade. We show that turbulent flow with a Kolmogorov spectrum can be easily recovered by employing standard methods for reducing α away from shocks.

Key words: hydrodynamics – turbulence – methods: numerical – galaxies: clusters: intracluster medium – intergalactic medium.

1 INTRODUCTION

Turbulence in astrophysics is of key importance for the interstellar medium (ISM), intracluster medium (ICM) and intergalactic medium (IGM). Compressible, hydrodynamic turbulence is characterized by two dimensionless parameters, the Mach number $\mathcal{M} \equiv V/c_s$ and the Reynolds number (Stokes 1851; Reynolds 1883)

$$\mathcal{R}_e \equiv \frac{VL}{\nu}, \qquad (1)$$

where V is the flow velocity, L is a typical length-scale, ν is the viscosity of the fluid and c_s is the sound speed. Physically, these parameters estimate the relative importance of each of the terms in the Navier–Stokes equations – the Mach number specifies the ratio of the inertial term, $(\boldsymbol{v}\cdot\nabla)\boldsymbol{v}$, to the pressure term, $\nabla P/\rho$, while the Reynolds number specifies the ratio of the inertial term to the viscous dissipation term, $\nu\nabla^2\boldsymbol{v}$. Mathematically, these two parameters – along with the boundary conditions and driving – entirely characterize the flow.

Given the importance of turbulence in theoretical models, it is crucial that agreement can be found between codes used for simulations of the ISM and ICM/IGM. Several comparison projects have been published recently comparing simulations of both decaying (Kitsionas et al. 2009) and driven (Price & Federrath 2010a) supersonic turbulence relevant to molecular clouds. However, fewer calculations appropriate to the ICM or IGM have been performed. In a recent preprint, Bauer & Springel (2011) have set out to extend the high Mach number comparisons to the mildly compressible, driven, subsonic turbulence thought to be appropriate to the ICM and IGM. In this case, the motions are comparable to or smaller than the sound speed, turbulent motions are dissipated by viscosity, and the flow is mainly characterized by the Reynolds number, similar to turbulence in the laboratory. In particular, it is well known from laboratory studies that the transition from laminar flow to fully developed turbulence only occurs once a critical Reynolds number is reached – for example, for Poiseuille flow (water flowing in a pipe) this is observed for $\mathcal{R}_e \gtrsim 2000$ (e.g. Reynolds 1895).

Since at low Mach number the Reynolds number controls not only the transition to turbulence, but also the character of such turbulence (e.g. the extent of the inertial range), it is critical to specify, or at least estimate, the Reynolds number employed in numerical simulations of turbulence in order to compare with the physical Reynolds numbers in the problems of interest. For the ISM, the physical Reynolds numbers are high [e.g. Elmegreen & Scalo (2004) estimate $\mathcal{R}_e \sim 10^5$–10^7 for the cold ISM] so the approach adopted has been to fix the Mach number and try to reach high numerical Reynolds numbers by minimizing numerical dissipation away from shocks. Estimates for $\mathcal{R}_e$ in the ICM/IGM are more difficult. Brunetti & Lazarian (2007) estimate $\mathcal{R}_e \sim 52$, but

⋆E-mail: daniel.price@monash.edu

© 2012 The Author
Monthly Notices of the Royal Astronomical Society © 2012 RAS

'rice (2012), MNRAS 420, L33

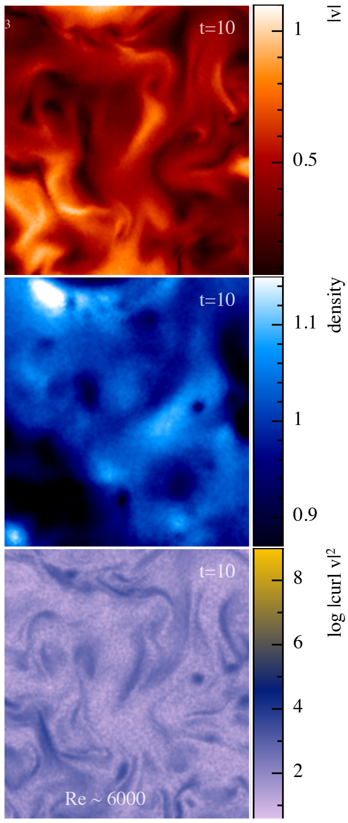

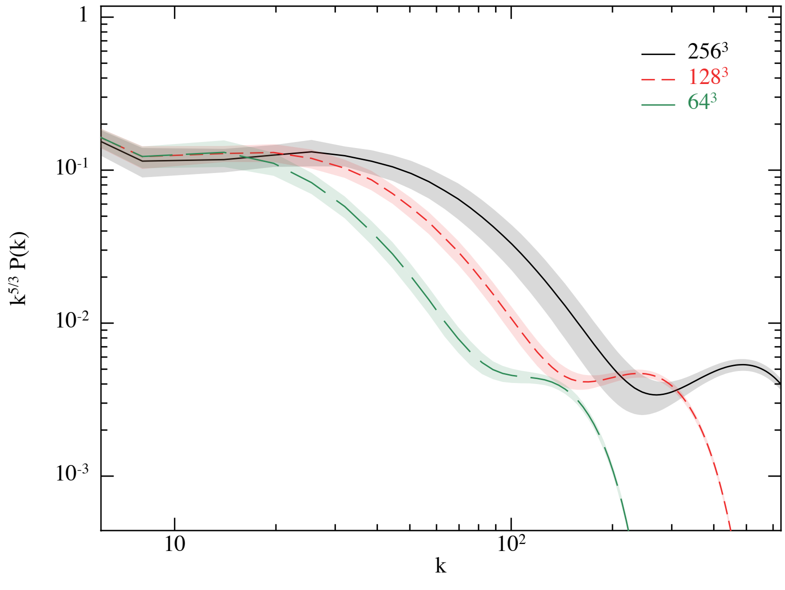

Figure 2. Time-averaged $k^{5/3}$-compensated power spectra from subsonic SPH turbulence calculations using the Morris & Monaghan (1997) viscosity switch at a resolution of 64^3, 128^3 and 256^3 particles, as indicated, for which the corresponding Reynolds numbers are $\sim$ 1500, 3000 and 6000, respectively. The shaded regions show the 1σ errors from the time-averaging. At the highest Reynolds numbers a Kolmogorov-like $k^{-5/3}$ slope is evident at large scales.

Are moving mesh schemes better, or just different?

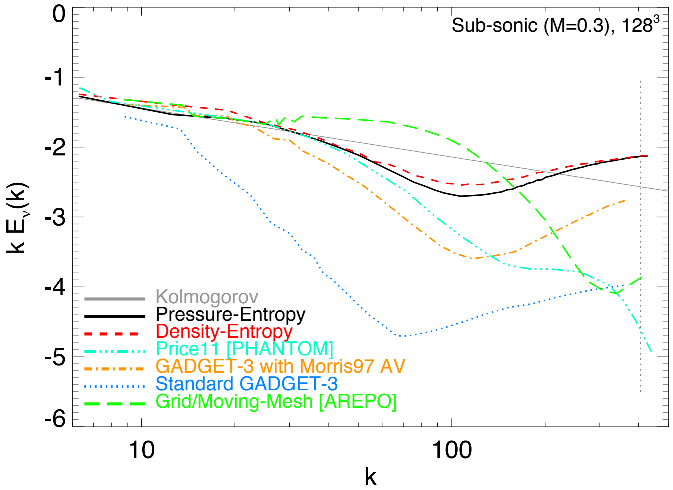

Figure 9. Velocity power spectrum in sub-sonic ($\mathcal{M} = 0.3$) driven, isothermal turbulence. Each simulation uses 128^3 particles and identical driving. We compare the analytic Kolmogorov inertial-range model, to that calculated from our standard density-entropy (Eq. 14) and pressure-entropy (Eq. 21) formulations. The mean softening length h is shown as the vertical dotted line. Both do well down to a few softenings, where they first fall below the analytic result (excess dissipation) then rise above (kernel-scale noise). The EOM choice has a weak effect on the results. We compare different SPH algorithms and codes (description in text); agreement is good where the same methods are used. The "PHANTOM" and "GADGET-3

Hopkins (2012) arXiv:1206.5006

"...deviations from Kolmogorov occur around the resolution limit, but are of a different character."

Summary: Advantages and disadvantages of SPH

Advantages:

- Resolution follows mass
- Zero dissipation until explicitly added
- Exact and simultaneous conservation of all physical quantities is possible
- Intrinsic remeshing procedure
- Does not crash

Disadvantages:

- Resolution follows mass
- Dissipation terms must be explicitly added to treat discontinuities
  - methods can be crude (need a good switch)
- Exact conservation no guarantee of accuracy
- Screw-ups indicated by noise rather than code crash

- ~~Historical difficulties incorporating magnetic fields (MHD)~~

Magnetic fields in SPH: recent progress

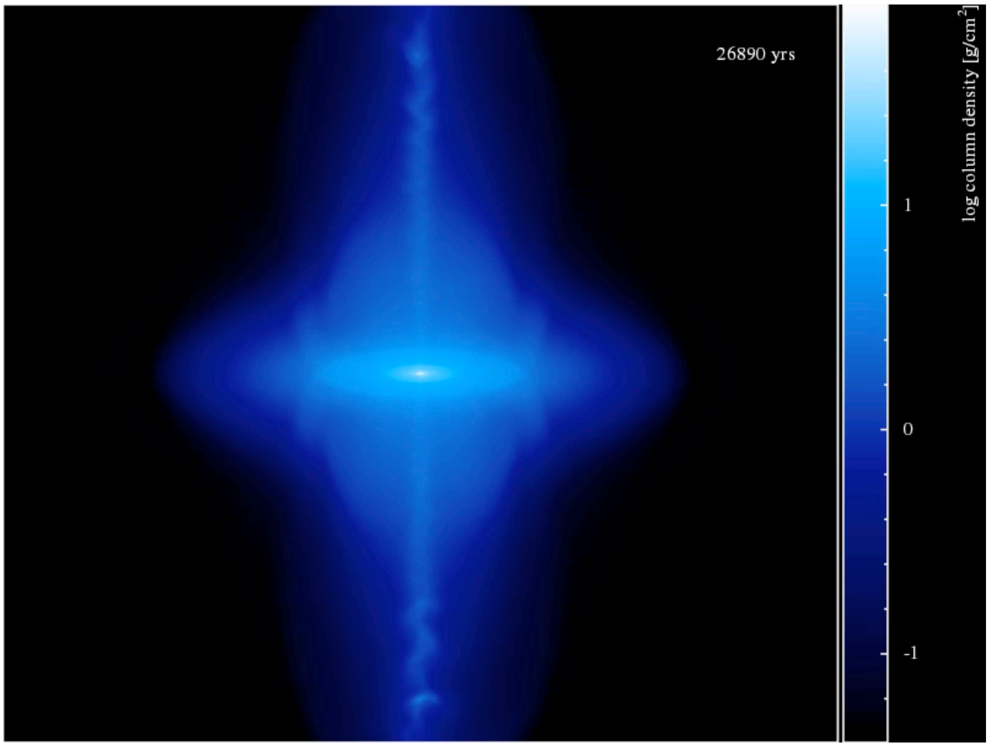

Price, Tricco & Bate (2012, MNRAS Lett.); Tricco & Price (2012, J. Comp. Phys.)

What is the future for SPH in numerical cosmology?

Recent key advances:

- Cullen & Dehnen (2010), Read & Heyfield (2011): state-of-the-art viscosity switches now capable of completely removing spurious effects of artificial viscosity away from shocks
- Dehnen & Aly (2012): pairing instability can be solved using Wendland kernels
- Tricco & Price (2012): New divergence cleaning scheme for SPMHD, we can do MHD in SPH for the first time with no limitations

Myths and misconceptions:

- Will carry on, it's the method everybody loves to hate
- SPH is deceptively simple to implement, much more difficult to master
- "Fundamental problems" have so far turned out to be rather elementary issues common to all numerical methods